

## **Responses to Anonymous Referee #2**

We thank the referee #2 for these helpful comments. Referee comments are numbered, with our responses, and any changes to the manuscript, subsequently given.

1) line 22: "2-22 month periods", what was the average period for all sites? Whether 2 or 22 months of data were available for a given station is highly relevant with regard to its representativeness. Please clarify in the abstract and in the text.

**The text and abstract now note that the average sampling period of sampling is 12 months.**

2) line 34: the term "residue" is rather confusing, especially if one sees later on in the text that it refers mainly to organic matter. I would suggest to find a different term.

**We have changed all mentions of 'residue' to 'residual' matter. We follow C. A. Brock et al.: Characteristics, sources, and transport of aerosols, ACP, 2011, figure 7, which notes of an aerosol "residual = un-specified mass (probably organic)".**

3) line 51, treatment of outliers: how were outliers processed? This line refers to a major sulphate event, and in the final section of the MS for several stations the authors describe the impact of dust events, major forest fires... How were these outliers dealt with? Depending on the duration of the sampling (see the first comment above), these outliers may have been not representative and strongly impact the mean aerosol concentration. A section should be added to discuss how frequent these outliers were, and how they were treated.

**These major events (e.g. dust storms, annual festivals) affect exposure and are thus included in the averages. These major events are described in detail in Section 5.3. Number of filters and date ranges are included for each site to assess representativeness.**

**For other instances of outlier data, we have added a new section (4.4), which describes major sources of uncertainty for chemical and physical measurements.**

4) lines 116-121: please highlight as a limitation that no data are available for Europe. This is a major spatial gap, despite data being openly available (e.g., chemical speciation data and nephelometry from the EMEP stations, stored in the EBAS database).

**We have added at the lines 169-171:**

**"Site selection prioritizes under-represented globally-dispersed, population-dense regions; no SPARTAN sites yet exist in Europe".**

5) line 135, what was the diameter of the filters, 47 mm?

**Thank you for noting this, we now state the 25mm filter diameter.**

6) line 155: were all the filters from all sites shipped to Dalhousie Univ. for analysis? Please describe

how filters were stored + transported to guarantee sample conservation, as this could be a major issue. How many filters/month were sampled, and how many in total per site? Please add a Table (even if in Supplementary material).

**Added 155-161: “As described by Snider et al (2015), loss rates of ammonium nitrate during passive air flow were an order of magnitude less than during active air flow. Thus the sampling protocol is designed to actively sample for one diurnal cycle and to avoid daytime sampling after collecting nighttime PM. Following the IMPROVE protocol (Hand and Malm, 2006), filters are transported at room temperature in sealed containers between measurement sites and the central SPARTAN laboratory at Dalhousie University, where analysis is conducted”.**

**The number of filters at each site is stated in Table 3. Line 151-2 states that one filter is sampled every 9 days. Thus there are typically 3 filters/month per site.**

7) line 298: please add a reference for the 0.18 coefficient applied to Na<sup>+</sup>

**We have added the reference Henning et al. (2003) to this line.**

8) line 320: please rename the fraction "residue matter" and state clearly from the beginning that it refers mainly to organics

**We have modified lines 247-249 to read**

**“Residual matter, which is treated as mainly organics, is estimated by subtracting dry inorganic mass (IN) and its associated water (referenced to our weighing conditions of  $35 \pm 5$  % RH) from total PM<sub>2.5</sub> mass”**

9) section 4.10: this entire section is very descriptive, but hardly any interpretation of the results is provided.

**We have moved this descriptive overview to section 5.1 to emphasize that it is intended to provide context for interpretation of specific site characteristics in the rest of section 5.**

10) line 357: this result is surprising for Beijing: even despite the influence of dust storms, a major urban area like Beijing should have a high Zn/Al ratio (high anthrop. influence). Why is this not the case? Could it be due to the potential lack of representativeness of the samples, linked to how outliers were dealt with? Please discuss and clarify in the text.

**We compared our ratios with previous work (Yang et al. 2011), that found a ratio of Zn:Al 0.67, which remains lower than compared with Hanoi and Dhaka. The moderate Zn:Al ratio could reflect the sampling location to the west of the city, upwind of many traffic sources. We have commented further on this in section 5.3.1 (previously 4.12.1), lines 468-473:**

**“The mean PM<sub>2.5</sub> Zn:Al ratio is lower than other large cities (0.51) likely due to larger fraction of natural dust sources and the sampling location in the northwest quadrant of the city, upwind of many traffic sources. The lowest coarse-mode Zn:Al mass ratios are observed in April 2014 (0.07)**

**and April 2015 (0.06) during the annual Yellow dust storm season. This is balanced by urban dust sources throughout the year, in agreement with Lin et al. (2015) who found evidence of high CM in industrial areas of Beijing”.**

11) line 376, 60% in Kanpur: if RM is so high in Kanpur it implies that CM will be very low, which seems surprising for an Indian city. Could this be because sampling took place during the monsoon season, maybe? This refers again to the temporal representativeness of the sampling. Some of the chemical composition results seem unexpected, please include a section discussing the potential sources of uncertainty, e.g. sampling period, filter transport, technical issues during sampling... What could have gone wrong, with such a dispersed network of stations?

**The RM in Kanpur is consistent with previous measurements of organics and RM in Kanpur. From section 5.3.6 (lines 566- 569):**

**“Notably the combined OM + unknown fractions from these previous two studies account for two thirds of aerosol mass, 58% for Behera and Sharma (2010) and 63% for Ram et al. (2012), similar to our 59% RM estimate”.**

**We also added a new section 4.4 (lines 339-346) to describe our sources of uncertainty regarding loss of semivolatiles:**

**“Of concern is the loss of semivolatiles after sampling. In the laboratory we reduce semivolatile loss by storing filters in closed containers. For time spent in the field, we examined the trend in PM<sub>2.5</sub> mass and ANO<sub>3</sub> from the first filter sampled (54 day residence time in instrument) through the last filter sampled (negligible residence time in instrument). Statistically insignificant trends were found for both PM<sub>2.5</sub> ( $-0.09 \pm 0.46 \mu\text{g m}^{-3}/\text{position}$ ) and ANO<sub>3</sub> ( $0.06 \pm 0.15 \mu\text{g m}^{-3}/\text{position}$ ) providing confidence in retention of semivolatiles on filters in the cartridge”.**

12) line 394, strong correlation between ASO<sub>4</sub> and ANO<sub>3</sub>: this is unexpected due to the thermal instability of ANO<sub>3</sub> in summer (when formation of ASO<sub>4</sub> is highest). On an annual basis both components might correlate, but not on a monthly basis. Please clarify.

**We clarified that ammonium and sulfate correlate well, but make no claims that ammonium nitrate correlates well with ammonium sulfate. ( $r^2 < 0.15$ ).**

13) section 4.11: this section is very unclear, what studies are the authors comparing their SPARTAN results with? Please specify. What are "study A" and "Study B" in the Figure?

**We have removed the terms “Study A” and “Study B”. The first sentence of this section (lines 433-434) was modified to**

**“We compare SPARTAN PM<sub>2.5</sub> speciation with one or two previous studies available from the literature (Prior Study in figure 3) and focus on collocated relative PM<sub>2.5</sub> composition of major species within the last 10 years.”**

14) line 417: "expectation that RM is organic", this is not an expectation, it is a definition of the

SPARTAN methodology (given that all other components are already accounted for)

**We modified lines 450-452 to now read:**

**“...SPARTAN measurements of RM appear to be predominantly organic in nature”.**

15) line 410: "10-30%", this is an overall limitation of the work: because such a broad range of station types, geographical regions and locations is used, the results also become rather broad and non-specific. E.g., stating that  $\text{ASO}_4$  contributes with 10-30% to  $\text{PM}_{2.5}$  mass is not a very specific result, it could represent almost anywhere in the world. Therefore, please state this limitation in the intro or results section, and extract the use of this kind of very global data, e.g. probably (in my opinion) for modelling studies, etc. What is the ultimate purpose of this work? Otherwise it becomes simply a descriptive manuscript.

**The ultimate purpose of work is to describe the initial results about  $\text{PM}_{2.5}$  concentrations from around the world. Due to the variability of PM components at each location, we provide broad concentration ranges when describing the SPARTAN project as a whole. We are developing modelling studies to further interpret the measured composition.**

**We have modified Lines 18-21 of the Abstract to read:**

**“The Surface PARTICulate mAtter Network (SPARTAN) is a long-term project that includes characterization of chemical and physical attributes of aerosols from filter samples collected worldwide. This manuscript discusses the ongoing efforts of SPARTAN to define and quantify major ions and trace metals found in fine particulate matter ( $\text{PM}_{2.5}$ )”.**

**Lines 122-123 in the Introduction now reads:**

**“We discuss the ongoing efforts of the SPARTAN project to quantify major ions and trace metals found in aerosols worldwide”.**

16) section 4.12.1: same issue as above, please discuss the relative contribution of natural and anthropogenic dust in Beijing. The large number of samples available (100) should allow for this kind of interpretation.

**We elaborate on the Zn:Al ratio to understand the relative contribution of natural and anthropogenic dust. We are currently preparing a manuscript that characterizes source attribution of different chemicals and elements. Lines 470-475:**

**“The mean  $\text{PM}_{2.5}$  Zn:Al ratio is lower than other large cities (0.51) likely due to larger fraction of natural dust sources and the sampling location in the northwest quadrant of the city, upwind of many traffic sources. The lowest coarse-mode Zn:Al mass ratios are observed in April 2014 (0.07) and April 2015 (0.06) during the annual Yellow dust storm season. This is balanced by urban dust sources throughout the year, in agreement with Lin et al. (2015) who found evidence of high CM in industrial areas of Beijing”**

17) line 445: due to volatilization but also to the fact that the authors are comparing their results with those from different periods in time, in the other studies.

**We now note different sampling periods. Lines 478-480:**

**“SPARTAN ANO<sub>3</sub> concentrations (8.5%) are relatively higher than most other locations, though lower than either previous study (11-12 %), possibly due to different sampling periods”.**

18) line 520, "organic matter burning": this is another example of a potential outlier. In addition, it would be useful if the authors could add somewhere in the text a brief assessment of major common emission sources, e.g., biomass combustion, agriculture, natural dust... This would help to integrate the results from the different sites rather than simply state ranges of chemical components (e.g., ASO<sub>4</sub> = 10-30%) which don't provide much specific information.

**These major common emission sources are described at the start of Section 2. We are preparing a modelling comparison manuscript to more quantitatively assess emission sources.**

19) line 572: festival in Israel, another probable outlier

**We agree this festival is an unusual event. However, it is an event that affects ambient PM. We moved discussion of this event into a separate paragraph.**

20) line 691: black carbon should be equivalent black carbon

**Updated and corrected, thank you.**

21) line 697: "3-year span", please clarify that this is not a continuous monitoring period in all sites, but instead a sequence of consecutive 4-month (approx) periods in different stations. This is a very big difference.

**We have modified this to read**

**“We report ongoing measurements of fine particulate matter (PM<sub>2.5</sub>), including compositional information, in 13 locations in two month or greater intervals all within a three-year span (2013-2016)”**

22) Conclusions: the conclusions section is again very descriptive, it is rather a summary. Actual conclusions and applications for their data should be extracted by the authors.

**We have revised this section to further develop specific conclusions.**

23) As proposed above, a reference to major common emission sources could be added (this is slightly hinted at in paragraph 7369-744).

**We attempt to tailor emission sources to each SPARTAN location. More general land use references include Latham et al (2014) and O:C characteristics from Canagaratna et al. (2015).**

### **Responses to Anonymous Referee #3**

We thank the referee #3 for these helpful comments. Referee comments are numbered, with our responses, and any changes to the manuscript, subsequently given.

1) The introduction is a bit disjointed. As a suggestion, I recommend moving the paragraph that begins on line 102 to line 78 (becomes 2nd paragraph), followed by the paragraph starting on line 93, with the sentence starting as “Furthermore, no global. . .” on line 80-82 added to the end, so that the RH effects are included in 1 paragraph. The rest of the paragraph (line 83-91) can become the 4th paragraph, followed by the paragraph at line 114, finishing with the paragraph on line 121. The order of the discussion would then be 1) Health (2) Chemical composition (3) Humidity effects (4) Satellites (5) SPARTAN (6) Purpose

**Thank you, we have adjusted the order of paragraphs to reflect your suggestions.**

2) A difficulty with the current organization of the paper is that the section on hygroscopicity comes before aerosol composition such that aerosol components (like ASO<sub>4</sub>) are being discussed before the reader knows how the authors define them. It would help to follow the development of the method if the description of the assumed aerosol components came first, and the kappa development followed. I recommend switching the order of section 3 (aerosol hygroscopicity) and section (4) PM<sub>2.5</sub> aerosol composition. Also, define a new section for mass speciation results (4.10 and onward). In accord with this reorganizing, switch the order of Figure 1 and 2, and Tables 1 and 2.

**Thank you, we have arranged sections 3 and 4 as you have suggested, and the corresponding tables and figures. We have also moved lines 158-162 to the beginning of the new Section 5.**

*Specific comments follow:*

3) I recommend instead of “ammonium sulfate”, referring to ASO<sub>4</sub> as “ammoniated sulfate” because the definition doesn’t necessarily assume fully neutralized ammonium sulfate (1.375\*SO<sub>4</sub>).

**Thank you, we have made the suggested change throughout text.**

4) Please point out that PM<sub>2.5</sub> and PM<sub>10</sub> are gravimetrically weighed. Line 19: I’m not sure what “maximize the chemical and physical information” means? It seems like the project is characterizing the chemical and physical attributes of aerosols from filter samples.

**We have removed this sentence to (lines 20-23)**

**“Our methods infer the spatial and temporal variability of PM<sub>2.5</sub> in a cost-effective manner. Gravimetrically-weighed filters represent multi-day averages of fine particulate matter (PM<sub>2.5</sub>), with a collocated nephelometer sampling air continuously.”**

5) Line 24: Define AERONET for first time use.

**Done, this is now referred to Aerosol Robotic Network**

6) Line 28: Consider replacing “baseline” with “background” or “rural/remote”.

**We now use your suggestion of using ‘background’.**

7) Line 34: What RH?

**We have appended “at 35% RH” to the end of sentence**

8) Line 41: Define IMPROVE for first time use.

**We now refer to IMPROVE as Interagency Monitoring of Protected Visual Environments**

9) Line 42: From the slope, which network had higher mass?

**Our values were higher. Modified sentence to read (lines 42-45)**

**“Comparison of SPARTAN versus coincident measurements from the Interagency Monitoring of Protected Visual Environments (IMPROVE) network at Mammoth Cave yielded...”**

10) Line 51: Change “included” to “including”

**Done**

11) Line 51: What was the standard deviation?

**The standard deviation of kappa is 0.04, which has now been included.**

12) Line 96: Define CSN

**Done. CSN is now defined as Chemical Species Network.**

13) Line 97: Define AIM

**Done. AIM is now defined as the Aerosol Inorganic Model.**

14) Line 99: Define kappa

**We have rephrased lines 102-105 to**

**“More recently Petters and Kreidenweis (2007, 2008, 2013) have developed  $\kappa$ -Kohler theory, which assigns individual hygroscopicity parameters  $\kappa$  to all major components,**

**from insoluble crustal materials to sea-salt.”**

15) Line 126: “As a function of chemical speciation” seems redundant.

**Rephrased lines 126-129 to**

**“Section 3 defines categories of aerosol types (crustal and residue material, black carbon, ammonium nitrate, ammoniated sulfate, sea salt, and trace metal oxides) as a function of specific chemical species.”**

16) Line 134: Provide years of sampling

**Added at line 136-137 “across 13 SPARTAN sites, between 2013 and 2016”**

17) Line 147: Define PM10

**Rephrased lines 149-150 to**

**“Air samples first pass through a bug screen and then a greased impactor plate in order to remove particles larger than 10  $\mu\text{m}$  in diameter”.**

18) Line 157: Is PM2.5 here gravimetric mass or summed constituents?

**Rephrased, and moved to beginning of Section 5 (lines 366):**

**“Gravimetrically-weighed PM<sub>2.5</sub> concentrations within the period June 2013 to February 2016 span an order of magnitude, from 9  $\mu\text{g m}^{-3}$  (e.g. Atlanta) to nearly 100  $\mu\text{g m}^{-3}$  (Kanpur)”.**

19) Line 166: Add “with other networks”

**Changed lines 169-170 to**

**“The sites of Atlanta and Mammoth Cave are included for instrument inter-comparison purposes with other networks”.**

20) Line 173: This sentence implies that surface reflectance is used to obtain all of the following constituents, not just black carbon.

**Thank you. We corrected lines 177-178 to read**

**“These filters are subsequently analyzed for water-soluble ions, trace metals, and surface reflectance to obtain black carbon”.**

21) Line 189: Add “K+” here, assuming that the potassium discussed later is from the IC.



**Done.**

22) Line 235: Define 1:1 v/v notation

**We have amended lines 295-296 to**

**“A 1:1 volume ratio with water as RH approaches 0% yields  $a = 2$ ”**

23) Line 239: Replace the IMPROVE convention with a reference, perhaps Pitchford et al., 2007. (“Revised algorithm for estimating light extinction from IMPROVE particle speciation data”, JAWMA, 57, 1326-1336).

**Thank you, we have now included this reference on line 299.**

24) Line 273: Check notation in table 2 and make sure it is the same as in the text for each species.

**We now define NaCl as ‘Sea Salt’ or ‘SS’ throughout text.**

25) Line 295: This is a little confusing. I assume based on Table 2 that the authors are saying  $0.1 * CM = Al + Fe + Mg$  but it isn't immediately clear from this sentence.

**Modified lines 222-223 to**

**“we generalize that natural CM is approximately  $10x[Al + Fe + Mg]$ ”**

26) Line 318: Point out that RM is assumed to be organic matter.

**Have rephrased lines 247-248 to**

**“Residue matter, which is treated as mainly organics, is estimated by subtracting dry inorganic mass (IN) ...”**

27) Line 342: Define NO<sub>x</sub> first use

**Modified line 383 to “...variation in NH<sub>3</sub> and NO<sub>x</sub> (NO + NO<sub>2</sub>) sources”**

28) Line 357: Coarse Zn:Al ratios are discussed throughout the paper but from the composition section, it seems like only PM<sub>2.5</sub> composition was analyzed. Was the coarse mode speciated also measured?

**We did measure coarse-mode speciation but focused on fine-mode evaluation for this paper. An upcoming manuscript will contain coarse-mode data.**

29) Line 395: What was the site average? It would be useful to add a column to table 3 with this information for each site.

**We have now provided correlations between ammonium and nitrate in table 3.**

30) Line 404: What is the significance of “Study A” and “Study B”? Why are they referred to in this way?

**Both are now labeled “Prior study”.**

31) Line 429: There are several instances when the values in the text are not exactly what are reported in the figures. (PM<sub>2.5</sub> is 69 in text, 70 in figure)

**Thank you. We have corrected values to reflect our most recent findings.**

32) Line 463: 25% in texts, 24% in figure.

**Fixed, thank you.**

33) Line 472: 17 in text, 18 in figure.

**Fixed, thank you.**

34) Line 483: Recommend discussing the sites in the same order as displayed in the figure.

**Certain sites did not have comparison figures associated. We aim to order the sites from most to least data available.**

35) Line 506: PM<sub>c</sub> notation has not been used previously.

**Have included in Methodology section (lines 150-153):**

**Aerosols are collected in sequence on a preweighed Nuclepore filter membrane (8 μm, SPI) that removes coarse-mode aerosols with diameters from 2.5 - 10 μm in diameter (PM<sub>c</sub>), while fine aerosols (PM<sub>2.5</sub>) are then collected on pre-weighed PTFE filters (2 μm, SKC).**

36) Line 514: 55% in text 59% in figure. 18% in text, 19 in figure, 7% in text, 7.4% in figure.

**Discrepancies have been fixed, thank you. Concentrations have also been updated reflecting new data acquired since submissions.**

37) Line 554: Does total mass here refer to PM<sub>2.5</sub>?

**Yes. Modified line 616-617 to read “...and total mass of PM<sub>2.5</sub> ( $r^2 = 0.76$ , slope = 1.12).”**

38) Line 556: add “respectively” to these comparisons so the reader knows which is which. The order of the comparison switched for CM (note 11% in text, 10% in figure) and EBC.

**Added the word ‘respectively’ to lines 617-619**

**“Differences between IMPROVE vs. SPARTAN are small for ASO4 (36% vs. 33%), ANO3 (2.4% vs. 1.2%), CM (7% vs. 11%), and EBC (3.0% vs. 5.6%), respectively”.**

39) Line 570: Does “total aerosol mass” here refer to PM2.5?

**Yes. Replaced “total mass” with “total PM2.5 mass”.**

40) Line 578: Again P<sub>m</sub>c notation used here.

**P<sub>m</sub>c is now defined in methodology section, line 151.**

41) Line 592: And the Butler et al value of 55%.

**Modified lines 632-635 to**

**“SPARTAN component fractions in Atlanta are also consistent with respect to Butler et al. (2003); components CM (12% vs. 10%), ASO4 (23% vs. 28%), ANO3 (3.5% vs 4%) and RM and OM (48% vs 55%) closely match, except for EBC (11% vs. 3%), perhaps reflecting different time periods.”.**

42) Line 594: CM 10% in text, 11 in figure, ASO4: 21% in text, 24% in figure; ANO3: 3% in text, 3.6% in figure.

**These discrepancies have been fixed, thank you. Concentrations have also been updated reflecting new data acquired since submissions.**

43) Line 610: Replace BC with EBC. Also, 9% in text, 10% in figure.

**Discrepancy has been fixed, thank you.**

44) Line 629: Does this Zn:Al ratio refer to PM2.5 or PM10?

**Now makes reference to PM2.5.**

45) Line 663: What were the average mass scattering efficiencies applied here, and were they consistent with major mass compositions during the same time periods? There are periods with fairly high biases between the mass estimates. Are the assumptions of constant mass and density appropriate during these periods, based on composition data?

**We tried to clarify at the start of this section that composition-specific  $\kappa_v$  values are used.**

46) Line 678: 0.71 in text, 0.70 in Figure

**Fixed, thank you.**

*Tables and Figures*

47) Line 1112: Another reason for switching the order of the hygroscopicity and aerosol composition sections would be that the species in Table 1 are not defined until Table 2. Switching the order would help to interpret Table 1.

**We have changed the order of the tables as suggested.**

48) Line 1112: Are the values of PBW averaged across all sites?

**In table 3, PBW is averaged across sites as a percent of total mass. However, it is reported as absolute mass for individual sites.**

49) Line 1121: There are some discrepancies with notation of species mass in this table and the text. I recommend using “sea salt” instead of “NaCl” since it is used in the text (line 279). Also,  $0.18[\text{Na}]_{\text{ss}}$  used in the table but  $0.18[\text{Na}]$  used in text (line 287). Define RH, X. Define SSR.

**We have now changed NaCl to SS or Sea Salt throughout the text, and added SS subscript. X, SSR, and RH have been defined as well.**

# Variation in Global Chemical Composition of PM<sub>2.5</sub>: Emerging Results from SPARTAN

1  
2  
3  
4  
5 Graydon Snider<sup>1</sup>, Crystal L. Weagle<sup>2</sup>, Kalaivani K. Murdymootoo<sup>1</sup>, Amanda Ring<sup>1</sup>, Yvonne  
6 Ritchie<sup>1</sup>, Emily Stone<sup>1</sup>, Ainsley Walsh<sup>1</sup>, Clement Akoshile<sup>3</sup>, Nguyen Xuan Anh<sup>4</sup>, Rajasekhar  
7 Balasubramanian<sup>5</sup>, Jeff Brook<sup>6</sup>, Fatimah D. Qonitan<sup>7</sup>, Jinlu Dong<sup>8</sup>, Derek Griffith<sup>9</sup>, Kebin He<sup>7</sup>,  
8 Brent N. Holben<sup>10</sup>, Ralph Kahn<sup>9</sup>, Nofel Lagrosas<sup>11</sup>, Puji Lestari<sup>6</sup>, Zongwei Ma<sup>12</sup>, Amit Misra<sup>13</sup>,  
9 Leslie K. Norford<sup>14</sup>, Eduardo J. Quel<sup>15</sup>, Abdus Salam<sup>16</sup>, Bret Schichtel<sup>17</sup>, Lior Segev<sup>18</sup>, S.N.  
10 Tripathi<sup>12</sup>, Chien Wang<sup>19</sup>, Chao Yu<sup>20</sup>, Qiang Zhang<sup>7</sup>, Yuxuan Zhang<sup>7</sup>, Michael Brauer<sup>21</sup>, Aaron  
11 Cohen<sup>22</sup>, Mark D. Gibson<sup>23</sup>, Yang Liu<sup>18</sup>, J. Vanderlei Martins<sup>24</sup>, Yinon Rudich<sup>16</sup>, Randall V.  
12 Martin\*<sup>1,2,25</sup>  
13  
14

---

\* Corresponding author email: [graydon.snider@dal.ca](mailto:graydon.snider@dal.ca) or [randall.martin@dal.ca](mailto:randall.martin@dal.ca) phone: 902-494-1820, fax: 902-494-5191

## *Affiliations*

<sup>1</sup>Department of Physics and Atmospheric Science, Dalhousie University, Halifax, Canada

<sup>2</sup>Department of Chemistry, Dalhousie University, Halifax, Canada

<sup>3</sup>Department of Physics, University of Ilorin, Ilorin, Nigeria

<sup>4</sup>Institute of Geophysics, Vietnam Academy of Science and Technology, Hanoi, Vietnam

<sup>5</sup>Department of Civil and Environmental Engineering, National University of Singapore

<sup>6</sup>Department of Public Health Sciences, University of Toronto, Toronto, Ontario, Canada M5S 1A8

<sup>7</sup>Faculty of Civil and Environmental Engineering, ITB, JL. Ganesha No.10, Bandung 40132, Indonesia

<sup>8</sup>Center for Earth System Science, Tsinghua University, Beijing, China

<sup>9</sup>Council for Scientific and Industrial Research (CSIR), Pretoria, South Africa

<sup>10</sup>Earth Science Division, NASA Goddard Space Flight Center, Greenbelt, Maryland, USA

<sup>11</sup>Manila Observatory, Ateneo de Manila University campus, Quezon City, Philippines

<sup>12</sup>School of Environment, Nanjing University, Nanjing, China.

<sup>13</sup>Center for Environmental Science and Engineering, Indian Institute of Technology Kanpur, India

<sup>14</sup>Department of Architecture, Massachusetts Institute of Technology, Cambridge, MA, 02139, USA

<sup>15</sup>UNIDEF (CITEDEF-CONICET) Juan B. de la Salle 4397 – B1603ALO Villa Martelli, Buenos Aires, Argentina

<sup>16</sup>Department of Chemistry, University of Dhaka, Dhaka - 1000, Bangladesh

<sup>17</sup>Cooperative Institute for Research in the Atmosphere, Colorado State, Colorado, USA

<sup>18</sup>Department of Earth and Planetary Sciences, Weizmann Institute, Rehovot 76100, Israel

<sup>19</sup>Center for Global Change Science, Massachusetts Institute of Technology, Cambridge, MA, 02139, USA

<sup>20</sup>Rollins School of Public Health, Emory University, 1518 Clifton Road NE, Atlanta, GA 30322, United States

<sup>21</sup>School of Population and Public Health, University of British Columbia, Vancouver, British Columbia, Canada

<sup>22</sup>Health Effects Institute, 101 Federal Street Suite 500, Boston, MA 02110-1817, USA

<sup>23</sup>Department of Process Engineering and Applied Science, Dalhousie University, Halifax, Canada,

<sup>24</sup>Department of Physics and Joint Center for Earth Systems Technology, University of Maryland, Baltimore County, Baltimore, Maryland, USA

<sup>25</sup>Harvard-Smithsonian Center for Astrophysics, Cambridge, MA 02138, USA

## Abstract

The Surface PARTiculate mAtter Network (SPARTAN) is a long-term project that includes characterization of chemical and physical attributes of aerosols from filter samples collected worldwide. This manuscript discusses the ongoing efforts of SPARTAN to define and quantify major ions and trace metals found in fine particulate matter (PM<sub>2.5</sub>). Our methods infer the spatial and temporal variability of PM<sub>2.5</sub> in a cost-effective manner. Gravimetrically-weighed filters represent multi-day averages of PM<sub>2.5</sub>, with a collocated nephelometer sampling air continuously. SPARTAN instruments are paired with AERosol RObotic NETwork (AERONET) sun photometers to better understand the relationship between ground-level PM<sub>2.5</sub> and columnar aerosol optical depth (AOD).

We have examined the chemical composition of PM<sub>2.5</sub> at 12 globally dispersed, densely populated urban locations and a site at Mammoth Cave (US) National Park used as a background comparison. Each SPARTAN location has so far been active between the years 2013 and 2016 over 2 to 26 month periods, with an average period of 12 months per site. These sites have collectively gathered over 10 site-years of quality aerosol data. The major PM<sub>2.5</sub> constituents across all sites (relative contribution ± SD) are ammoniated sulfate (20% ± 11%), crustal material (13.4% ± 9.9%), black carbon (11.9% ± 8.4%), ammonium nitrate (4.7% ± 3.0%), sea salt (2.3% ± 1.6%), trace element oxides (1.0% ± 1.1%), water (7.2% ± 3.3%) at 35% RH, and residual matter (40% ± 24%).

Analysis of filter samples reveals that several PM<sub>2.5</sub> chemical components varied by more than an order of magnitude between sites. Ammoniated sulfate ranges from 1.1 μg m<sup>-3</sup> (Buenos Aires, Argentina) to 17 μg m<sup>-3</sup> (Kanpur, India [dry season]). Ammonium nitrate ranged from 0.2 μg m<sup>-3</sup> (Mammoth Cave, in summer) to 6.8 μg m<sup>-3</sup> (Kanpur, dry season). Equivalent black carbon ranged from 0.7 μg m<sup>-3</sup> (Mammoth Cave) to over 8 μg m<sup>-3</sup> (Dhaka, Bangladesh and Kanpur, India). Comparison of SPARTAN versus coincident measurements from the Interagency Monitoring of Protected Visual Environments (IMPROVE) network at Mammoth Cave yielded a high degree of consistency for daily PM<sub>2.5</sub> ( $r^2 = 0.76$ , slope = 1.12), daily sulfate ( $r^2 = 0.86$ , slope = 1.03) and mean fractions of all major PM<sub>2.5</sub> components (within 6%). Major ions generally agree well with previous studies at the same urban locations (e.g. sulfate fractions agree within 4% for eight out of 11 collocation comparisons). Enhanced anthropogenic dust fractions in large urban areas (e.g. Singapore, Kanpur, Hanoi and Dhaka) are apparent from high Zn:Al ratios.

The expected water contribution to aerosols is calculated via the hygroscopicity parameter  $\kappa_v$  for each filter. Mean aggregate values ranged from 0.15 (Ilorin) to 0.28 (Rehovot). The all-site parameter mean is 0.20 ± 0.04. Chemical composition and water retention in each filter measurement allows inference of hourly PM<sub>2.5</sub> at 35% relative humidity by merging with nephelometer measurements. These hourly PM<sub>2.5</sub> estimates compare favorably with a beta attenuation monitor (MetOne) at the nearby US embassy in Beijing, with a coefficient of variation  $r^2 = 0.67$  ( $n = 3167$ ), compared to  $r^2 = 0.62$  when  $\kappa_v$  was not considered. SPARTAN continues to provide an open-access database of PM<sub>2.5</sub> compositional filter information and hourly mass collected from a global federation of instruments.

## 60 1. Introduction

61

62 Fine particulate matter with a median aerodynamic diameter less than, or equal to, 2.5  $\mu\text{m}$   
63 ( $\text{PM}_{2.5}$ ), is a robust indicator of premature mortality (Chen et al., 2008; Laden et al., 2006).

64 Research on long-term exposure to ambient  $\text{PM}_{2.5}$  has documented serious adverse health effects,  
65 including increased mortality from chronic cardiovascular disease, respiratory disease, and lung  
66 cancer (WHO, 2005). Outdoor fine particulate matter ( $\text{PM}_{2.5}$ ) is recognized as a significant air  
67 pollutant, with an Air Quality Guideline set by the WHO at 10  $\mu\text{g m}^{-3}$  annual average (WHO,  
68 2006). Many regions of the world far exceed these long-term recommendations (Brauer et al.,  
69 2015; van Donkelaar et al., 2015), and the impact on health is substantial. The 2013 Global  
70 Burden of Disease estimated that outdoor  $\text{PM}_{2.5}$  caused 2.9 million deaths (3 % of all deaths) and  
71 70 million years of lost healthy life on a global scale (Forouzanfar et al., 2015). Atmospheric  
72 aerosol is also the most uncertain agent contributing to radiative forcing of climate change  
73 (IPCC, 2013). Aerosol mass and composition also play a critical role in atmospheric visibility  
74 (Malm et al. 1994). Additional observations are needed to improve the concentration estimates  
75 for  $\text{PM}_{2.5}$  as a global risk factor, and to better understand the chemical components and sources  
76 contributing to its formation.

77

78 The chemical composition of  $\text{PM}_{2.5}$  offers valuable information to identify the  
79 contributions of specific sources, and to understand aerosol properties and processes that could  
80 affect health, climate and atmospheric conditions. Spatial mapping of aerosol type and  
81 composition using satellite observations and chemical transport modelling can help elucidate the  
82 global exposure burden of fine particulate matter composition (Kahn and Gaitley, 2015;  
83 Lelieveld et al., 2015; Patadia et al., 2013; Philip et al., 2014a), however ground-level sampling  
84 remains necessary to evaluate these estimates and provide quantitative detail. Furthermore, the  
85 long-term health impacts of specific chemical components are not well understood (e.g. Lepeule  
86 et al., 2012). The health-related impacts of specific PM composition have been reviewed  
87 previously (Lippmann, 2014). Although  $\text{PM}_{2.5}$  composition can be implicated in the variance  
88 observed in cardiovascular health effects, there is insufficient long-term  $\text{PM}_{2.5}$  characterization  
89 for adequate health impact assessments of specific aerosol mixtures (e.g. Bell et al., 2007). More  
90 generally, urban  $\text{PM}_{2.5}$  speciation is not yet consistently characterized on a global scale.  
91 Continental sampling has been conducted in North America (Hand et al., 2012) and Europe  
92 (Putaud et al., 2004, 2010), however there remains a need for a global network that consistently  
93 measures  $\text{PM}_{2.5}$  chemical composition in densely populated regions.

94

95 No global  $\text{PM}_{2.5}$  protocol exists for relative humidity (RH) filter equilibration. The U.S.  
96 EPA measurements are between 30-40% RH, European measurements are below 50% RH, and  
97 different protocols exist elsewhere. Ambient humidity affects the relationship of dry  $\text{PM}_{2.5}$  with  
98 satellite observations of aerosol optical depth. Aerosol water also influences the relationship  
99 between dry  $\text{PM}_{2.5}$  and aerosol scatter. A large body of literature has examined the relationship  
100 of aerosol composition with hygroscopicity (e.g. IMPROVE (Hand et al., 2012; IMPROVE,  
101 2015), **Chemical Species Network** (CSN) (Chu, 2004; USEPA, 2015), ISORROPIA (Fountoukis  
102 and Nenes, 2007), and **Aerosol Inorganic Model** (AIM) (Wexler and Clegg, 2002)). **More**  
103 **recently Petters and Kreidenweis (2007, 2008, 2013) have developed  $\kappa$ -Kohler theory, which**  
104 **assigns individual hygroscopicity parameters  $\kappa$  to all major components, from insoluble crustal**  
105 **materials to sea-salt.** Mixed values can then be weighted by local aerosol composition.

106  
107 Ground-based observations of  $PM_{2.5}$  have insufficient coverage at the global scale to  
108 provide assessment of long-term human exposure. Satellite remote sensing offers a promising  
109 means of providing an extended temporal record to estimate population exposure to  $PM_{2.5}$  on a  
110 global scale, and especially for areas with limited ground-level  $PM_{2.5}$  measurements (Brauer et  
111 al., 2015; van Donkelaar et al., 2015). Even in areas where monitor density is high, satellite-  
112 based estimates provide additional useful information on spatial and temporal patterns in air  
113 pollution (Kloog et al., 2011, 2013; Lee et al., 2012). However, there are outstanding questions  
114 about the accuracy and precision with which ground-level aerosol mass concentrations can be  
115 inferred from satellite remote sensing. Standardized  $PM_{2.5}$  measurements, collocated with  
116 ground-based measurements of aerosol optical depth, are needed to evaluate and improve  $PM_{2.5}$   
117 estimates from satellite remote sensing. To meet these sampling needs, the ground-based  
118 network SPARTAN (Surface PARTiculate mAtter Network) is designed to evaluate and enhance  
119 satellite-based estimates of  $PM_{2.5}$  by measuring fine particle aerosol concentrations and  
120 composition continuously over multi-year periods at sites where aerosol optical depth is also  
121 measured (Holben et al., 1998; Snider et al., 2015). The network includes air filter sampling and  
122 nephelometers that together provide long-term and hourly  $PM_{2.5}$  estimates at low RH (35%).  
123

124 We discuss the ongoing efforts of the SPARTAN project to quantify major ions and trace  
125 metals found in aerosols worldwide. Section 2 describes the methodology used to infer  $PM_{2.5}$   
126 composition. Section 3 defines categories of aerosol types (crustal and residual material, black  
127 carbon, ammonium nitrate, ammoniated sulfate, sea salt, and trace metal oxides) as a function of  
128 specific chemical species. Section 4 describes the implementation of sub-saturated  $\kappa$ -Kohler  
129 theory to estimate aerosol water content based on aerosol compositional information. Section 5  
130 compares relative aerosol composition with that reported in available literature, and assesses the  
131 general consistency of our findings across all sites. Section 6 evaluates hourly  $PM_{2.5}$  estimates  
132 (35% RH) at Beijing with a beta attenuation monitor at the US Embassy.  
133

## 134 2. Overview of Methodology

135

136 SPARTAN has been collecting  $PM_{2.5}$  on PTFE filters for at least two months, across 13  
137 SPARTAN sites, between 2013 and 2016, with an average period of 12 months per site. Snider  
138 et al. (2015) provide an overview of the SPARTAN PM observation network, the cost-effective  
139 sampling methods employed and post sampling instrumental methods of analysis. Each site  
140 utilizes a combination of continuous monitoring by nephelometry and mass concentration via  
141 filter-based sampling. Nephelometer scatter is averaged to hourly intervals at three wavelengths  
142 (457nm, 520nm, 634nm), and converted to 550 nm via a fitted Angstrom exponent. Total scatter  
143 is proportional to  $PM_{2.5}$  mass and volume (Chow et al., 2006). Hence we provide dry (35% RH)  
144 hourly  $PM_{2.5}$  estimates by combining scatter at 550 nm at ambient RH with filter mass and  
145 chemical composition information used to determine water content as described below.  
146

147 Briefly, filter-based measurements are collected with an AirPhoton SS4i automated air  
148 sampler. Each sampler houses a removable filter cartridge that protects seven sequentially active  
149 25 mm diameter filters plus a field blank. Air samples first pass through a bug screen and then a  
150 greased impactor plate to remove particles larger than 10  $\mu\text{m}$  in diameter. Aerosols are collected  
151 in sequence on a preweighed Nuclepore filter membrane (8  $\mu\text{m}$ , SPI) that removes coarse-mode



152 aerosols with diameters from 2.5 - 10  $\mu\text{m}$  in diameter ( $\text{PM}_{10}$ ), while fine aerosols ( $\text{PM}_{2.5}$ ) are then  
153 collected on pre-weighed PTFE filters (2  $\mu\text{m}$ , SKC). For each filter, sampling is timed at regular,  
154 staggered 24-hour intervals throughout a 9-day period. Sampling ends for each filter at 09:00  
155 when temperatures are low, to reduce loss of semi-volatile components. As described by Snider  
156 et al (2015), loss rates of ammonium nitrate during passive air flow were an order of magnitude  
157 less than during active air flow. Thus the sampling protocol is designed to actively sample for  
158 one diurnal cycle and to avoid daytime sampling after collecting nighttime PM. Following the  
159 IMPROVE protocol (Hand and Malm, 2006), filters are transported at room temperature in  
160 sealed containers between measurement sites and the central SPARTAN laboratory at Dalhousie  
161 University, where analysis is conducted.

162  
163 Site locations are designed to sample under a variety of conditions, including biomass  
164 burning, (e.g. West Africa and South America), biofuel emissions (e.g. South Asia), monsoonal  
165 conditions (e.g. West Africa and Southeast Asia), suspended mineral dust (e.g. West Africa and  
166 the Middle East) and urban crustal material. Each SPARTAN site provides a representative  
167 example of local and regional conditions in highly populated areas. Site selection prioritizes  
168 under-represented globally-dispersed, population-dense regions; no SPARTAN sites yet exist in  
169 Europe. The sites of Atlanta and Mammoth Cave are included for instrument inter-comparison  
170 purposes with other networks.

### 171 2.1. Filter weighing

172 Filters (PTFE, capillary) are both pre and post-weighed in triplicate using a Sartorius Ultramicro  
173 balance with 0.1  $\mu\text{g}$  precision. Gravimetric weighing is performed in a cleanroom facility at  $35 \pm$   
174 5% RH and 20-23°C. A total of 497 quality-controlled filters have been weighed across all  
175 SPARTAN sites. The median collected material on sampled filters, as well as the lower and  
176 upper quintiles (in parentheses), are 72 (42, 131)  $\mu\text{g}$  for Teflon and 90 (44, 154)  $\mu\text{g}$  for  
177 Nuclepore. The combined uncertainty ( $\pm 2\sigma$ ) of quality-assured single filter PM mass  
178 measurements is  $\pm 4.0 \mu\text{g}$ . These filters are subsequently analyzed for water-soluble ions, trace  
179 metals, and surface reflectance to obtain black carbon.

### 180 2.2. Equivalent Black Carbon (EBC)

181 We define the equivalent black carbon (EBC) as the black carbon content of PTFE filters derived  
182 via surface reflectance  $R$  using the Diffusion Systems Smoke Stain Reflectometer EEL 43M  
183 (Quincey et al., 2009) as further discussed in Sect. 4.6. We use the term equivalent black carbon  
184 following the recommendation of Petzold et al. (2013) for data derived from optical absorption  
185 methods.

### 186 2.3. Trace metals

187 To maximize the information extracted from the filters, each one is cut in half with a ceramic  
188 blade following approaches similar to Zhang et al. (2013) and Gibson et al. (2009). One filter  
189 half is analyzed for relevant trace metals, i.e. crustal components Zn, Mg, Fe, and Al. We digest  
190 this half by adding it to 3.0 mL of 7% trace metal grade nitric acid, similar to Fang et al. (2015).  
191 The acid/filter combination is boiled at 97°C for 2 hours, and the liquid extract is submitted for  
192 quantitative analysis via inductively coupled plasma mass spectrometry (ICP-MS, Thermo  
193 Scientific X-Series 2).

## 194 2.4. Water soluble ions

195 Water-soluble ions  $\text{NO}_3^-$ ,  $\text{SO}_4^{2-}$ ,  $\text{NH}_4^+$ ,  $\text{K}^+$ ,  $\text{Na}^+$  are detected using the second filter half. The filter  
196 is spiked with 120  $\mu\text{L}$  of isopropyl alcohol and immersed in 2.9 mL of 18 M $\Omega$  Milli-Q water.  
197 Filters and liquid extracts are sonicated together for 25 min before being passed through a 0.45  
198  $\mu\text{m}$  membrane filter to remove larger matrix components. Extractions are analyzed by ion  
199 chromatography (IC) via a Thermo Dionex ICS-1100 instrument (anions) and a Thermo Dionex  
200 ICS-1000 (cations) instrument (Gibson et al., 2013a, 2013b).  
201

## 202 3. $\text{PM}_{2.5}$ aerosol composition

203  
204 Section 2 defined the methodology of basic physical and chemical properties obtained in  
205 SPARTAN filters. Section 3 describes the chemical definitions used to infer each chemical  
206 component as discussed in turn below. Table 1 contains a summary of equations and  
207 accompanying references used to quantify SPARTAN  $\text{PM}_{2.5}$  chemical composition.

### 208 3.1. Sea Salt (SS)

209 We take 10% of  $[\text{Al}]$  to be associated with Na and remove this crustal sodium component  
210 (Remoundaki et al., 2013). Sea salt is then represented as  $2.54[\text{Na}^+]_{\text{ss}}$  to account for the  
211 associated  $[\text{Cl}^-]$  (Malm et al., 1994).

### 212 3.2. Ammonium nitrate ( $\text{ANO}_3$ )

213 We treat all nitrate as neutralized by ammonium as  $\text{NH}_4\text{NO}_3$ . The corresponding mass of  $\text{ANO}_3$   
214 is a 1:1 molar ratio of  $\text{NH}_4:\text{NO}_3$ , or  $1.29[\text{NO}_3^-]$  based on molecular weight.

### 215 3.3. Sodium sulfate ( $\text{Na}_2\text{SO}_4$ )

216 Sodium sulfate is treated as a fraction of measured sodium,  $0.18[\text{Na}^+]_{\text{ss}}$  (Henning et al., 2003);  
217 however, it contributes negligibly to total aerosol mass ( $< 0.1\%$ ) at all sites.

### 218 3.4. Ammoniated sulfate ( $\text{ASO}_4$ )

219 Ammonium not associated with nitrate, and sulfate not associated with sodium, are assumed to  
220 mutually associate as a mixture of  $\text{NH}_4\text{HSO}_4$  and  $(\text{NH}_4)_2\text{SO}_4$ .

### 221 3.5. Crustal material (CM)

222 Crustal material consists of re-suspended road dust, desert dust, soil, and sand. Following the  
223 elemental composition of natural desert dusts by Wang (2015), we generalize that natural CM is  
224 approximately  $10 \times [\text{Al} + \text{Fe} + \text{Mg}]$ . Aluminum, iron, and magnesium are chosen due to their  
225 collectively consistent composition in natural mineral dust and frequency above detection limit  
226 ( $> 95\%$ ). Silicon is not available. Titanium was found not to contribute significantly ( $< 1\%$ ) to  
227 CM mass.

### 228 3.6. Equivalent Black Carbon (EBC)

229 The amount of EBC carbon ( $\mu\text{g}$ ) is logarithmically related to concentration, as determined by  
230 relative surface reflectance  $R/R_0$ . For a given exposed filter area, absorption cross-section and  
231 light path, reflectance is related to concentration via

$$[\text{EBC}] = \frac{-A}{qv} \ln\left(\frac{R}{R_0}\right) \quad \text{Eq. 1}$$

232 where  $v$  is volume of air (0.9 to 5.8 m<sup>3</sup>),  $A$  is the filter surface area (3.1 cm<sup>2</sup>), and  $q$  is the product  
 233 of the effective reflectivity path  $p$  and mass-specific absorption cross section  $\sigma_{SSR}$  (cm<sup>2</sup>/μg). The  
 234 absorption coefficient  $\sigma_{SSR}$  used here is 0.06 cm<sup>2</sup>/μg based on prior literature (Barnard et al.,  
 235 2008; Bond and Bergstrom, 2006), adjusted to the 620 nm detection peak of the SSR. The  
 236 effective light path  $p$  here is taken to be 1.5 for our thick PTFE filters (e.g. Taha et al., 2007). We  
 237 treat water uptake by EBC as negligible.

### 238 3.7. Trace elemental oxides (TEO)

239 Trace elemental oxides are the summation of oxides for all measured ICP trace elements, and  
 240 make up a negligible portion of total mass (< 1%). We include these concentrations for  
 241 completeness. Water uptake by TEO is treated as negligible.

### 242 3.8. Particle-bound water (PBW) associated with inorganics

243 We estimate the water-mass uptake for the inorganic chemical components of sea salt (SS),  
 244 ammonium nitrate (ANO<sub>3</sub>) and ammoniated sulfate (ASO<sub>4</sub>). The mass of particle-bound water  
 245 (PBW) associated with chemical component  $X$  is

$$PBW_X = [X] \kappa_{m,x} \frac{\text{RH}}{100 - \text{RH}} \quad \text{Eq. 2}$$

246 The total mass of inorganic (IN) PBW is then  $PBW_{\text{IN}} = \sum_X PBW_X$ .

### 247 3.9. Residual matter (RM)

248 Residual matter, which is treated as mainly organics, is estimated by subtracting dry inorganic  
 249 mass (IN) and its associated water (referenced to our weighing conditions of 35 ± 5 % RH) from  
 250 total PM<sub>2.5</sub> mass:

$$\text{RM}_{35\%} = \text{PM}_{2.5,35\%} - [\text{IN}] - [\text{PBW}_{\text{IN}}] \quad \text{Eq. 3}$$

251 Negative RM<sub>35%</sub> values are retained if reconstructed inorganic mass at 35% RH exceeds total  
 252 PM<sub>2.5</sub> by less than 10%, otherwise values are flagged and excluded from the mass average.  
 253 Negative values occur, on average, 2% of the time. Water-free RM (0% RH) is estimated by  
 254 subtracting organic-associated PBW using an estimated hygroscopic parameter  $\kappa_{m,\text{RM}} = 0.1$  as  
 255 discussed in section 4.

## 257 4. Aerosol hygroscopicity

258  
 259 We apply the single-parameter measure of aerosol hygroscopicity ( $\kappa$ ) developed by Petters  
 260 and Kreidenweis (2007, 2008, 2013) to represent the contribution of water uptake by individual  
 261 components. The  $\kappa$  parameter is defined from 0 (insoluble materials) to greater than 1 for sea  
 262 salt. Although initially developed for supersaturated CCN conditions, hygroscopic parameters  $\kappa$   
 263 have been more recently used in sub-saturated conditions (Chang et al., 2010; Dusek et al., 2011;  
 264 Giordano et al., 2013; Hersey et al., 2013). For particle diameters that dominate the mass fraction  
 265 of PM<sub>2.5</sub> (larger than 50 nm), the difference in  $\kappa$  between CCN and sub-saturated aerosols is

266 small (Dusek et al., 2011). The water retention of internal mixtures of aerosol components is  
 267 often predicted within experimental error (Kreidenweis et al., 2008). Aged, polarized organic  
 268 material, which is a major component of PM<sub>2.5</sub>, shows comparable growth factors both in super-  
 269 and sub-saturated regions (Rickards et al., 2013).

270  
 271 The volume hygroscopicity parameter  $\kappa_v$  is defined as a function of particle volume  $V$  and  
 272 water activity  $a_w$

$$\frac{1}{a_w} = 1 + \kappa_v \frac{V_d}{V_w} \quad \text{Eq. 4}$$

273 where  $V_d$  and  $V_w$  are the dry particulate matter and water volumes, respectively. To a first-order  
 274 approximation  $a_w = \text{RH}/100$ . Aerosol volume growth is related via  $\kappa$  and RH by defining  $f_v(\text{RH})$   
 275 as the humidity-dependent ratio of wet and dry aerosol volume:

$$f_v(\text{RH}) \equiv \frac{V_{tot}}{V_d} = \frac{V_d + V_w}{V_d} = a + \kappa_v \frac{\text{RH}}{100 - \text{RH}} \quad \text{Eq. 5}$$

276 Combining the previous equations and relating to a diameter  $D$  growth factor ( $GF \equiv D/D_d$ ) yields

$$GF = \left( a + \kappa_v \frac{\text{RH}}{100 - \text{RH}} \right)^{1/3} \quad \text{Eq. 6}$$

277 where  $a = 1$ , except for sea salt as discussed in Sect. 3.1. Reliable estimates of  $\kappa_v$  are available  
 278 for individual components (*c.f.* Table 2).

279  
 280 The next sections outline how we apply  $\kappa$  to represent mass and volume hygroscopic growth  
 281 in major hygroscopic aerosol components. Four components directly contribute to water uptake:  
 282 ammonium nitrate (ANO<sub>3</sub>), ammoniated sulfate (ASO<sub>4</sub>), sea salt (SS), and organics. We treat  
 283 black carbon (EBC), crustal material (CM), and trace oxides (TEO) as non-hygroscopic. We  
 284 evaluated inorganic component growth curves using the AIM model (Wexler and Clegg, 2002)  
 285 for RH = 10 – 90% except for sea salt, which included RH = 0%. Hygroscopic parameters were  
 286 matched to modeled fits. Aerosols are treated as internally mixed, without deliquescence or  
 287 efflorescence points, as discussed further below.

#### 288 4.1. Inorganic behavior

289 Figure 1 shows the hygroscopic growth for inorganics. The  $\kappa_v$  value of 0.51 for ASO<sub>4</sub>  
 290 best matches the AIM model over RH = 10-90% and is similar to the  $GF$ -derived  $\kappa_v = 0.53$   
 291 estimated by Petters and Kreidenweis (2007). Our AIM-derived ANO<sub>3</sub> growth curve is smaller  
 292 than ASO<sub>4</sub>, at  $\kappa_v = 0.41$ . Although both ammonium compounds share the same  $GF = 1.6$  at RH =  
 293 85% (Sorooshian et al., 2008), ANO<sub>3</sub> is less hygroscopic at lower RH.

294  
 295 Sea salt accounts for a small fraction of aerosol mass over land, however its hydrophilic  
 296 nature makes it significant for water retention. A 1:1 volume ratio with water as RH approaches  
 297 0% (Kreidenweis et al., 2008) yields  $a = 2$  (Eq. 2 and 3). A hygroscopic constant  $\kappa_v = 1.5$  then  
 298 best fits AIM from the deliquescence point up to 90% RH.

299

300 We follow the widely used convention (e.g. Pitchford et al. (2007)) that  $PM_{2.5}$  under  
 301 variable sub-saturated RH does not exhibit deliquescent phase transitions. There is compelling  
 302 evidence to adopt smooth hygroscopic growth curves. Various experiments show sub-  
 303 micrometer, internally mixed aerosols will not deliquesce as readily as pure compounds. For  
 304 example, Badger et al. (2006) observed  $ASO_4$  aerosol deliquescence is clearly inhibited by the  
 305 presence of humic acids. A smooth growth curve has been observed over the range  $RH = 10 -$   
 306  $85\%$  for ambient aerosols at Jungfraujoch (Swietlicki et al., 2008). Analysis of submicron aerosol  
 307 mixtures consisting of SS,  $ASO_4$ ,  $ANO_3$ , and levoglucosan also showed no apparent phase  
 308 transition (Svenningsson et al., 2006).

#### 309 4.2. Organic matter behavior

310 Identifying a representative organic hygroscopic parameter is challenging, as many volume  
 311 growth curves are available based on a variety of laboratory experiments and field campaigns.  
 312 Organic composition varies by site, and by season. The Appendix table A1 contains a collection  
 313 of hygroscopic parameters from the literature. Values for  $\kappa_{v,OM}$  range from 0 to 0.2. We choose a  
 314 single  $\kappa_{v,OM}$  value based on the oxygen/carbon ratio (O:C), which is a function of oxidation,  
 315 hence age of the organics. Generally O:C ratios are between 0.2 – 0.8 in urban environments  
 316 (Rickards et al., 2013). We select an O:C ratio of 0.5 to represent the populated nature of  
 317 SPARTAN sites (e.g. Robinson et al., 2013). This corresponds to an organic parameter of  
 318  $\kappa_{v,OM} = 0.1$  for a variety of organic mixtures (Jimenez et al., 2009).

#### 319 4.3. Aerosol water in multi-component systems

320 Mass-based hygroscopic water uptake  $\kappa_m$  is more convenient than  $\kappa_v$  to estimate water  
 321 retention in gravimetric analysis. The parameters  $\kappa_v$  and  $\kappa_m$  are related by water-normalized  
 322 density,  $\kappa_{m,X} = \kappa_{v,X}/\rho_X$ . Table 2 contains  $\kappa_v$  values identified for major aerosol chemical  
 323 components and densities. For a multi-component system we estimate aerosol water mass using a  
 324 mass-weighted combination of  $\kappa_m$  values:

$$\kappa_{m,tot} = \frac{1}{M} \sum_X m_X \kappa_{m,X} \quad \text{Eq. 7}$$

325 Mass calculations are used to determine residual aerosol mass as described in Sect 4.9.  
 326 Estimates of total water uptake by volume are applied to aerosol light scatter in Sect. 5. The  
 327 volume parameter  $\kappa_{v,tot}$  is similarly determined by a linear combination of volume-weighted  
 328 components  $X$  (e.g. Bezantakos et al., 2013):

$$\kappa_{v,tot} = \frac{1}{V} \sum_X v_X \kappa_{v,X} \quad \text{Eq. 8}$$

329 The hygroscopic growth of  $ASO_4$  and organic mixtures are treated as linear combinations of pure  
 330 compounds (Robinson et al., 2013). Errors in aerosol water uptake are less significant in mixtures  
 331 than for individual species due to dilution effects (Kreidenweis et al., 2008). For ambient aerosols,  
 332 empirically measured  $\kappa_{v,tot}$  usually lies between 0.14 and 0.39 (Carrico et al., 2010).  
 333

#### 334 4.4. Sources of Uncertainty

335 Uncertainty in atmospheric PM<sub>2.5</sub> concentrations can be separated into air volume and PM<sub>2.5</sub>  
336 mass. We estimated total flow volume variance to be  $\pm 10\%$ , while  $2\sigma$  pre and post gravimetric  
337 mass measurement varied by a combined  $\pm 4 \mu\text{g}$ . Characterization of hourly PM<sub>2.5</sub> uncertainties  
338 can be found in Appendix A2.

339  
340 Of concern is the loss of semivolatiles after sampling. In the laboratory semivolatile loss  
341 is inhibited by storing filters in closed containers. As discussed in Section 2, the sampling  
342 protocol is designed to minimize semi-volatile loss. We tested the retention of semivolatile  
343 material in the field by examining the trend in PM<sub>2.5</sub> and ANO<sub>3</sub> mass from the first filter sampled  
344 (54 day residence time in instrument) through the last filter sampled (negligible residence time in  
345 instrument). Statistically insignificant trends were found for both PM<sub>2.5</sub> ( $-0.09 \pm 0.46 \mu\text{g m}^{-3}$   
346 <sup>3</sup>/position) and ANO<sub>3</sub> ( $0.06 \pm 0.15 \mu\text{g m}^{-3}$ /position) providing confidence in retention of  
347 semivolatiles on filters in the cartridge.

348  
349 Other uncertainties include absolute equivalent black carbon mass due to the reflectivity  
350 path  $p$  ( $\pm 30\%$ ) and absorption cross section  $\sigma$  ( $\pm 30\%$ ), which combine to in quadrature  $\pm 42\%$ .  
351 Trace metal recovery yields were tested using a sequential second digestion with 20% nitric acid.  
352 Each acid-digested element was quantified by five dilutions of a 25 element standard (25 – 500  
353 *ppb*) plus three internal calibration metals (Sc, In, Tb). The elemental comparison of crustal  
354 materials varies regionally (Wang, 2015), which contributes to CM uncertainty of  $\pm 30\%$  based  
355 on Al, Fe and Mg composition. Recovery of individual water-soluble elements was determined  
356 through 5-point anion and cation standards curves each with  $r^2 > 98\%$  and  $<10\%$  mass  
357 uncertainty for most elements at environmentally-relevant concentrations, including sulfate,  
358 nitrate, and ammonium. Based on lab filter spike tests, water-soluble ion extractions show  $> 95\%$   
359 extraction efficiency. Uncertainties of water-soluble ion yields are generally  $\pm 5\%$ , except when  
360 close to limit of detection (approximately  $0.1 \mu\text{g m}^{-3}$ , depending on filter sampling duration).  
361 Errors in the component values affect our estimate of  $\kappa_v$ , which will affect the inferred aerosol  
362 water. Network evaluation is ongoing task that will continue over time.

363

### 364 5. Mass speciation results

#### 365 5.1. Overview of PM<sub>2.5</sub> mass speciation

366 Gravimetrically-weighed PM<sub>2.5</sub> concentrations within the period June 2013 to February 2016  
367 span an order of magnitude, from under  $10 \mu\text{g m}^{-3}$  (e.g. Atlanta) to almost  $100 \mu\text{g m}^{-3}$  (Kanpur).  
368 Sites include a variety of geographic regions including partial desert (Ilorin, Rehovot, Kanpur),  
369 coastline (Buenos Aires, Singapore), and developing megacities (Dhaka). Table 3 and Figure 2  
370 contain the resulting PM<sub>2.5</sub> mass, composition, and location of each SPARTAN site. The mean  
371 SPARTAN composition over all sampling sites in descending concentration is 40% RM  
372 (primarily organic), 20% ASO<sub>4</sub>, 13% CM, 12% EBC, 4.7% ANO<sub>3</sub>, 2.3% SS and 1.0% TEO.

373

374 There is significant variation of relative and absolute speciation from these long-term  
375 averages. ASO<sub>4</sub> concentrations range from  $1 \mu\text{g m}^{-3}$  (Buenos Aires, summer) to  $17 \mu\text{g m}^{-3}$   
376 (Kanpur, dry season). The fraction of sulfate in PM<sub>2.5</sub> exhibits much weaker spatial variation (10-



377 30%) as increases in ASO<sub>4</sub> coincide with increases in total PM<sub>2.5</sub>. Hence locations with enhanced  
378 sulfate tend to have enhancements in other aerosol components.

379  
380 ANO<sub>3</sub> concentrations exhibit a larger spatial heterogeneity than sulfate. Absolute values  
381 range over 30-fold, from 0.2 μg m<sup>-3</sup> (Mammoth Cave, summer) to 6.8 μg m<sup>-3</sup> (Kanpur, dry  
382 season). Corresponding mass fractions are 7-8 % in Kanpur, Beijing, and Buenos Aires, and  
383 below 2% in Bandung. This heterogeneity reflects large spatial and temporal variation in NH<sub>3</sub>  
384 and NO<sub>x</sub> (NO + NO<sub>2</sub>) sources. There were noticeable seasonal increases in ANO<sub>3</sub> during  
385 wintertime periods in Beijing, Kanpur, and Dhaka, coinciding with lower temperatures.

386  
387 CM concentrations span an order of magnitude from 1.0 μg m<sup>-3</sup> (Atlanta) to 16 μg m<sup>-3</sup>  
388 (Beijing). The fraction of CM in PM<sub>2.5</sub> exhibits pronounced variation (5-25%). Except during  
389 dust storms, CM does not show clear patterns of temporal or regional variation. This could be  
390 explained by non-seasonal road dust, which may account for over 80% of CM in regions with  
391 heavy urban traffic (Huang et al., 2015).

392  
393 We used Zn:Al ratios to assess the relative importance of local road dust (*c.f.* Table 3).  
394 Aluminum is mostly natural in origin (Zhang et al., 2006) whereas Zn is primarily from tire wear  
395 (Begum et al., 2010; Councell et al., 2004). For example, ratios are above 3 for Dhaka and  
396 Hanoi, but less than 0.3 for Mammoth Cave and South Dekalb site (Atlanta). In fine-mode  
397 aerosols, the ratio tends to be highest in large cities distant from natural CM. In coarse-mode  
398 aerosols, a low Zn:Al ratio (< 0.1) indicates the aerosol CM component is dominated by regional  
399 dust.

400  
401 Absolute EBC spans an eight-fold concentration range from 1.1 μg m<sup>-3</sup> (Atlanta) to above 8  
402 μg m<sup>-3</sup> (Dhaka and Kanpur). Mass fractions of EBC ranged from 4% (Singapore) to 25%  
403 (Manila). Trace element oxide (TEO) material is mainly composed of Zn, Pb, Ni, Cu, and Ba,  
404 hence also derived mainly from anthropogenic sources. TEO contributes negligibly to total mass  
405 (1%), as expected. Sea salt remains a consistently small contributor (2%) to total mass, except  
406 for Buenos Aires and Rehovot (5-6%) due to coastal winds. Particle-bound water (PBW) mass at  
407 35% humidity is determined from the growth parameter κ<sub>m</sub>. PBW mass contribution is similar to  
408 EBC (7%). At low humidity, the combined mass of ANO<sub>3</sub>, EBC, TEO, sea salt, and PBW  
409 account for 15-35 % of aerosol mass.

410  
411 RM as inferred from mass reconstruction of inorganic compounds, PBW, and total filter-  
412 weighed mass is implicitly treated as the organic aerosol mass fraction. In terms of relative  
413 composition, RM spans a factor of two, from 30% mass in Buenos Aires to almost 60% in  
414 Kanpur. Temporal changes in RM tend to coincide with increases in ASO<sub>4</sub>, with an all-site r<sup>2</sup> =  
415 0.92. Although RM is not fully independent of ASO<sub>4</sub>, this relationship implies related sources.

416  
417 We interpret the abundance of water-soluble potassium K<sup>+</sup> relative to Al as an indicator of  
418 wood smoke (e.g. Munchak et al., 2011). K:Al ratios averaged over each site range from < 2  
419 (Mammoth Cave, Atlanta) to 16 (Kanpur), where combustion activity is apparent. Singapore was  
420 downwind of significant Indonesian forest fire smoke during its sampling period of Aug-Nov  
421 2015, averaging to K:Al = 13. The correlation between K:Al and RM across all SPARTAN sites  
422 is r<sup>2</sup> = 0.73, supporting the attribution of RM as mostly organic.

423  
424 Across all sites, coarse and fine mode mass fractions are approximately equal (0.50), with  
425 fractions ranging from below 0.40 (Hanoi, Buenos Aires, and Manila) to above 0.55 (e.g.  
426 Bandung, Kanpur, Atlanta, Mammoth Cave). The two size modes can be temporally correlated  
427 per site, though sometimes weakly, from  $r^2 = 0.15$  (Hanoi) to  $r^2 = 0.76$  (Rehovot). We observe  
428 strong temporal correlations between sulfate and ammonium in  $PM_{2.5}$  ( $r^2 = 0.72 - 0.99$ ). Nitrate  
429 and ammonium are less consistently related (Table 3), ranging from higher values in Singapore  
430 ( $r^2 = 0.66$ ), Kanpur ( $r^2 = 0.58$ ), Beijing ( $r^2 = 0.28$ ), to weaker values in Ilorin and Manila ( $r^2 <$   
431  $0.1$ ). The strength of correlations with ammonium could be influenced by excess ammonium  
432 relative to sulfate. The  $[NH_4^+]/[SO_4^{2-}]$  ratio in  $PM_{2.5}$  is 2.6 in Kanpur and 1.3 in Ilorin.

## 433 5.2. Collocation overview

434 We compare SPARTAN  $PM_{2.5}$  speciation with previous studies available from the literature  
435 and focus on collocated relative  $PM_{2.5}$  composition of major components within the last 10 years.  
436 TEO is omitted due to lack of significant mass contribution. Aerosol water content is also  
437 omitted as it was not directly measured in any of the collocation studies. If not provided, CM is  
438 treated as defined in Sect 4.5 where possible. Organic mass (OM) to organic carbon (OC) ratios  
439 are from Philip et al. (2014b) with updates from Canagaratna et al. (2015).

440  
441 Figure 3 provides an overview of the comparison studies organized by SPARTAN data  
442 availability. Only sampling at Mammoth Cave sampling was temporally coincident with the  
443 comparison data. SPARTAN compositional information is generally consistent with previous  
444 studies, considering inter-annual chemical variation and measurement uncertainty. For example,  
445 both SPARTAN and comparative studies find that  $PM_{2.5}$  is composed of between 10-30%  $ASO_4$   
446 and 5-20% CM for sampled sites. SPARTAN EBC mass fraction generally matches within 5  
447 percentage points of collocated studies, except for Bandung and Kanpur. SPARTAN and prior  
448 studies find that  $ANO_3$  is usually a small fraction of total mass, except at Beijing and Kanpur (7-  
449 8%) due to their high agricultural and industrial activity. All studies find that sea-salt is below  
450 3% of total mass. SPARTAN-derived RM has potentially the largest potential error, yet typically  
451 is consistent with the combined organic and unknown masses of other studies. This offers further  
452 evidence that SPARTAN measurements of RM are predominantly organic in nature.

## 454 5.3. Individual site characteristics

455 Below we discuss each site in more detail. We also examine how our chemical composition  
456 from a global array of sites relate to local anthropogenic activities and surrounding area.  
457 References to land type at specific sites are derived from Latham et al. (2014), unless otherwise  
458 indicated. The number of filters is given in parentheses.

### 460 5.3.1 Beijing, China ( $n = 114$ )

461 Beijing has attracted considerable attention for its air pollution (Chen et al., 2013).  
462 Agricultural areas to the west and the Gobi Desert to the north surround the city's 19 million  
463 dwellers. The SPARTAN air sampler is located on the Tsinghua University campus, 15 km  
464 northwest of the downtown center. This is our longest-running site, with 2.5 years of near-  
465 continuous sampling. It reports the third-highest  $PM_{2.5}$ , at  $69 \mu g m^{-3}$ , the third highest  $ASO_4$  ( $12$   
466  $\mu g m^{-3}$ ) and the highest CM ( $16 \mu g m^{-3}$ ) of all sites. The significant  $ANO_3$  ( $5.5 \mu g m^{-3}$ ) reflects



467 significant urban NO<sub>x</sub> near agricultural NH<sub>3</sub> sources. ANO<sub>3</sub> values were highest during winter,  
468 as expected from ammonium-nitrate thermodynamics. A high CM component in the springtime  
469 reflects regional, natural CM sources. The mean PM<sub>2.5</sub> Zn:Al ratio is lower than other large cities  
470 (0.51) likely due to larger fraction of natural dust sources and the sampling location in the  
471 northwest quadrant of the city, upwind of many traffic sources. The lowest coarse-mode Zn:Al  
472 mass ratios are observed in April 2014 (0.07) and April 2015 (0.06) during the annual Yellow  
473 dust storm season. This is balanced by urban dust sources throughout the year, in agreement with  
474 Lin et al. (2015) who found evidence of high CM in industrial areas of Beijing.

475  
476 *Beijing Comparison:* Relative masses in Beijing compare well with previous studies.  
477 SPARTAN ASO<sub>4</sub> (19%) is close to Yang et al. (2011) (17%) and Oanh et al. (2006) (20%)  
478 and the RM of 37% is similar to combined OM (33 and 29%) and unknown fractions (10 and  
479 24%) of comparison studies. SPARTAN ANO<sub>3</sub> concentrations (8.5%) are relatively higher  
480 than most other locations, though lower than either previous study (11-12%), possibly due to  
481 different sampling periods. CM is greater than Yang et al. (2011) (25% vs. 19%), and  
482 significantly higher than Oanh et al. (2006) (5%), potentially due to a difference in  
483 definitions.

### 484 485 **5.3.2 Bandung, Indonesia (n = 77)**

486 Bandung is located inland on western Java surrounded by a volcanic mountain range and  
487 agriculture (e.g. tea plantations). The sampler is located on the Institute of Technology Bandung  
488 campus, 5 km north of the city center. Almost two years of sampling have resulted in a mean  
489 PM<sub>2.5</sub> concentration of 31 μg m<sup>-3</sup>. Sea salt is low at this elevated (826 m) inland site. ANO<sub>3</sub> and  
490 CM levels are also low, but RM is moderately high compared with other sites, at 55%. This  
491 could be explained by large amounts of vegetative burning; organic PM<sub>2.5</sub> mass fractions can rise  
492 above 70% during combustion episodes (Fujii et al., 2014). Volcanic sources of sulfur, in  
493 addition to industrial sources, may explain the relatively higher ASO<sub>4</sub> compared with Manila or  
494 Dhaka (Lestari and Mauliadi, 2009). Influxes of volcanic dust from the Sinabang volcano from  
495 August – September 2014 (2000 km northwest of Bandung) could explain why coarse-mode  
496 Zn:Al ratios drop to 0.09 for this period compared to the annual mean of 0.21.

497  
498 *Bandung Collocation:* Bandung is a volcanically active area, so that composition, in  
499 particular ASO<sub>4</sub>, differs due to naturally variable circumstances. SPARTAN ASO<sub>4</sub> (21%) is  
500 higher than the 4% fraction reported by Lestari and Mauliadi (2009), but is identical with  
501 measurements by Oanh et al. (2006). SPARTAN EBC (13%) is less than either previous  
502 study (19% and 25%) and the more recent analysis of 19% BC (Santoso et al., 2013).  
503 SPARTAN ANO<sub>3</sub> is 2% by mass, lower than measured by Oanh et al. (2006) (13%) but  
504 similar to Lestari and Mauliadi (2009). Both of the earlier studies show lower RM fractions  
505 (36%, and 42%) compared with 54% RM in this study.

### 506 507 **5.3.3 Manila, Philippines (n = 63)**

508 Manila is a coastal city located in Manila Bay, adjacent to the South China Sea and  
509 surrounded by mountains. The sampling station, located at the Manila Observatory, is about 40  
510 m higher in altitude than the central city. The PM<sub>2.5</sub> concentrations at the observatory (18 μg m<sup>-3</sup>)  
511 are expected to be lower than in the main city, but still influenced by vehicular traffic, fuel  
512 combustion and industry (Cohen et al., 2009). Compared to the all-site average, the CM fraction

513 in Manila is typical (11%), but black carbon is twice as great (25%). The high EBC agrees with  
514 previous observations, attributable to a relatively high use of diesel engines (Cohen et al., 2002).

515  
516 *Manila Collocation:* SPARTAN fractions of ASO<sub>4</sub> and EBC are similar to Cohen et al.  
517 (2009). Our RM (43%) is lower than OM (57%), whereas SPARTAN CM was greater than  
518 Cohen et al. (2009). These differences could reflect sampling differences, or emission  
519 changes over the last decade.

#### 520 521 **5.3.4 Dhaka, Bangladesh (n = 41)**

522 Dhaka is a densely populated city (17,000 persons/km<sup>2</sup>) in a densely populated country  
523 (1,100 persons/km<sup>2</sup>). The sampler is situated in the heart of downtown Dhaka, on the University  
524 of Dhaka rooftop, and is influenced by air masses from the Indo Gangetic Plain (Begum et al.,  
525 2012). More than half the country is used for agricultural purposes (Ahmed, 2013). Local  
526 contributing PM<sub>2.5</sub> sources include coal and biomass burning, and heavy road traffic combustion  
527 products and dust (Begum et al., 2010, 2012). PM<sub>2.5</sub> concentrations are the fourth highest of any  
528 SPARTAN site, at 52 µg m<sup>-3</sup>. Dhaka has the second-highest absolute EBC of any site, at 8.4 µg  
529 m<sup>-3</sup>, which can be explained by the abundance of truck diesel engines (Begum et al., 2012). We  
530 estimate 41% of PM<sub>2.5</sub> in Dhaka is RM. Crop or bush burning on both local and regional scales  
531 contribute significantly to organics (Begum et al., 2012). The high mean PM<sub>2.5</sub> Zn:Al ratio of 3.4  
532 reflects a large contribution from urban traffic.

#### 533 534 **5.3.5 Ilorin, Nigeria (n = 40)**

535 Ilorin is located in a rural area with low-level agriculture and shrub vegetation. The sampler  
536 is sited on the university campus, 15 km east of the city of 500,000 people. Aerosol loadings  
537 have seasonal cycles from agricultural burning events and dust storms (Generoso et al., 2003).  
538 The RM accounted for two thirds of total PM<sub>2.5</sub> mass, among the largest, influenced by biomass  
539 burning. There is evidence of biomass burning in the PM<sub>2.5</sub> peak in late spring 2014, and again in  
540 2015. Lower ASO<sub>4</sub> (12%) compared to other SPARTAN sites reflects the sparse surrounding  
541 industry. CM levels are comparable to other locations, except during dust storms. During a dust  
542 storm (between April 14<sup>th</sup> - May 2<sup>nd</sup> 2015), CM increased to two thirds of PM<sub>2.5</sub> mass. The PM<sub>c</sub>  
543 Zn:Al ratio during the storm decreased to 0.01 versus 0.25 during non-storm days.

#### 544 545 **5.3.6 Kanpur, India (n = 33)**

546 Kanpur is a city of 2.5 million people. The sampler is located at the IIT Kanpur campus  
547 airstrip, about 10 km northwest of the city. The city lies in the Indo-Gangetic Plain, where  
548 massive river floodplains are used for agricultural and industrial activity (Ram et al., 2012). We  
549 sampled from December 2013 – May 2014, and September-November 2014, capturing one dry  
550 season. SPARTAN-measured PM<sub>2.5</sub> for this period was 99 µg m<sup>-3</sup>, the highest of any SPARTAN  
551 site, of which 59% is RM, 19% ASO<sub>4</sub>, and 7.4% ANO<sub>3</sub>. The absolute values of all three  
552 components are also the highest among those measured. Molar [NH<sub>4</sub><sup>+</sup>]:[SO<sub>4</sub><sup>2-</sup>] ratios are higher  
553 in Kanpur (2.6) than elsewhere. High background ammonia has been observed in the region  
554 from satellite (e.g. Clarisse et al., 2009) which could explain the high levels of ANO<sub>3</sub>. Wood  
555 smoke is apparent from the high K:Al ratio (16), associated with organic matter burning during  
556 winter dry months. We detected significant Zn concentrations (Zn:Al = 1.0), which is in  
557 agreement with Misra et al. (2014) observations of a tripling of zinc during anthropogenic  
558 sourced dust.

559  
560 *Kanpur Collocation:* Relative fractions among the major species CM, salt, ASO<sub>4</sub> & ANO<sub>3</sub> all  
561 match well with previous studies (Behera and Sharma, 2010; Chakraborty et al., 2015; Ram  
562 et al., 2012) that also sampled during winter dry seasons. Chakraborty et al. (2015) measured  
563 70% organic mass composition and found a combined mass of 28% for ASO<sub>4</sub> + ANO<sub>3</sub>  
564 compared to SPARTAN mass (26%). SPARTAN ASO<sub>4</sub> (19%) compares well to 13% of  
565 Ram et al. (2012) and 18% for Behera and Sharma (2010), and ANO<sub>3</sub> (7.4%) is close to  
566 previous values (6.1% and 6.6%). By comparison SPARTAN slightly overestimates EBC by  
567 4-6%. SPARTAN CM (4.8%) is lower than Behera and Sharma (2010) (10%). Notably the  
568 combined OM + unknown fractions from these previous two studies account for two thirds of  
569 aerosol mass, 58% for Behera and Sharma (2010) and 63% for Ram et al. (2012), similar to  
570 our 59% RM estimate. SPARTAN PM<sub>2.5</sub> concentrations, as well as RM, reach a maximum  
571 during the month of December. This is consistent with recent work (Villalobos et al., 2015),  
572 who attribute this increase to agricultural burning and stagnant air.

### 573 574 **5.3.7 Buenos Aires, Argentina (n = 31)**

575 Buenos Aires has a metropolitan population of 12 million. SPARTAN instruments are  
576 located on the urban CITEDEF campus 20 km west of the central downtown. The megacity, the  
577 southernmost in our study, is surrounded by grassland and farming on the west and the Atlantic  
578 Ocean on the east. The latter explains the relatively high proportion (6%) of sea salt. Total PM<sub>2.5</sub>  
579 (10 µg m<sup>-3</sup>) and relative RM (31%) are low compared with other large metropolitan areas, likely  
580 influenced by clean maritime air. In addition to sea salt and natural CM, the contribution of EBC  
581 is 17%, which could reflect significant local truck diesel combustion (Jasan et al., 2009).

### 582 583 **5.3.8 Rehovot, Israel (n = 30)**

584 Rehovot is located on a four-story rooftop on the Weizmann Institute campus, 11 km from  
585 the Mediterranean Sea and 20 km south of Tel Aviv. The city is surrounded by semi-arid, mixed-  
586 use cropland, and the region experiences occasional Saharan desert dust outbreaks. Typical PM<sub>2.5</sub>  
587 concentrations are low (16 µg m<sup>-3</sup>), with the composition in Rehovot consisting of 29% ASO<sub>4</sub>,  
588 and 20% CM. The RM fraction is smaller in Rehovot (16% total PM<sub>2.5</sub> mass) than at other  
589 SPARTAN sites. Aerosol sources in Israel include agriculture, desert dust, traffic and coal-based  
590 power plants (Graham et al., 2004). Relative sodium concentrations are high in Rehovot (4%),  
591 similar to Buenos Aires and Ilorin, and may include a contribution from dust.

592  
593 *Lag Ba'Omer festival:* We measured high ASO<sub>4</sub> concentrations on May 7-18, 2015, during  
594 which time a large number of bonfires were lit nearby. During the festival, over 75% of total  
595 aerosol mass came from ASO<sub>4</sub> + ANO<sub>3</sub>, leading to a brief doubling of the hygroscopic  
596 parameter κ<sub>v</sub>. We observed a K:Al ratio of 38 for May 6<sup>th</sup> of the festival, the highest for any  
597 single filter.

598  
599 *Saharan dust storm:* We had the opportunity to measure a severe dust storm in Rehovot from  
600 a filter sampling February 4-13, 2015. The coarse filter Zn:Al ratio dropped to 0.02 during  
601 the Saharan dust storm from the typical value of 0.3. On the coarse filter we obtained an  
602 absolute CM mass of 950 µg, which accounts for half of the collected mass during the storm.  
603 13% of dust storm PM<sub>c</sub> is combined sea salt, ANO<sub>3</sub>, and ASO<sub>4</sub>, leaving 35% RM. Although

604 this RM fraction may imply an incomplete CM extraction, it is possible that a significant  
605 portion of desert dust carries adsorbed organic material (Falkovich et al., 2004).

### 607 **5.3.9 Mammoth Cave NP, US (n = 19)**

608 The Mammoth Cave sampling site straddles National Park mountainous terrain to the north  
609 and east, with farmland to the south and west. It is about 35 km from the closest town, Bowling  
610 Green, KY, with about 50,000 residents. Sources of PM are expected to be non-local, hence we  
611 consider it our ‘background’ site.

612  
613 *Mammoth Cave National Park Collocation:* This temporary SPARTAN site was deployed  
614 for comparison with the IMPROVE network station (IMPROVE, 2015). Unique among our  
615 sites, sampling was temporally coincident with IMPROVE’s 1-in-3 day regimen. We  
616 obtained quality-controlled samples from June-August 2014. Temporal variation in daily  
617 values is consistent with IMPROVE for sulfate ( $r^2 = 0.86$ , slope = 1.03) and **total mass of**  
618 **PM<sub>2.5</sub> ( $r^2 = 0.76$ , slope = 1.12).** Differences between IMPROVE vs. SPARTAN are small for  
619 **ASO<sub>4</sub> (36% vs. 33%), ANO<sub>3</sub> (2.4% vs. 1.2%), CM (7% vs. 11%), and EBC (3.0% vs. 5.6%),**  
620 **respectively.** The combined OM + unknown + water fraction IMPROVE was 51%, similar to  
621 the SPARTAN RM mass fraction of 49%.

### 622 **5.3.10 Atlanta, US (n = 13)**

623 Atlanta represents a major urban area in a developed country. The temporary SPARTAN site  
624 was located at the South Dekalb supersite 15 km east of downtown Atlanta. Air sampling was  
625 performed for a 4-month period spanning winter to spring 2014. Over the past 10 years  
626 significant decreases in PM<sub>2.5</sub> have been observed here and across the eastern United States  
627 (Boys et al., 2014). The surrounding region is tree-covered or agricultural.

628  
629 *Atlanta (South Dekalb) Collocation:* Co-sampled filters from the Atlanta CSN station  
630 (USEPA, 2015) provide a comparison with the summer 2014 SPARTAN data. The EPA OM  
631 fraction (43%) agrees well with the SPARTAN mean **RM (48%).** **Crustal, SS, EBC and**  
632 **ASO<sub>4</sub> are within 2% relative to total composition.** SPARTAN component fractions in Atlanta  
633 **are also consistent with respect to Butler et al. (2003); components CM (12% vs. 10%),**  
634 **ASO<sub>4</sub> (23% vs. 28%), ANO<sub>3</sub> (3.5% vs 4%) and RM and OM (48% vs 55%) closely match,**  
635 **except for EBC (11% vs. 3%),** perhaps reflecting different time periods.

### 636 **5.3.11 Singapore, Singapore (n = 12)**

637  
638 Singapore is a densely populated coastal city-state at 7,770 people/km<sup>2</sup>. The sampler is  
639 located on a rooftop at the National University of Singapore (NUS), near the center of the city.  
640 Transportation is mixed-use, including taxis, rail, and bicycles, which may help explain the  
641 relatively low EBC and CM of 3%. Despite this, the Zn:Al ratio remains high at 1.5, implying a  
642 dominant traffic-based contribution to CM. SPARTAN instruments have observed significant  
643 biomass burning downwind from Indonesia, causing an increase in absolute PM<sub>2.5</sub> from 32 in  
644 August to 120 µg m<sup>-3</sup> in September 2015, as well as an increase in RM from 44% to 62%. The  
645 K:Al ratio steadily increased during this same period, from 7.2 (Jul 24 – Aug 2, 2015) to 17 – 24  
646 (Aug 11 – Sept 25).

650 **5.3.12 Hanoi, Vietnam (n = 10)**

651 Hanoi is an inland megacity surrounded by grassland and agriculture. The sampler itself is on  
652 a building rooftop at the Vietnam Academy of Science, 5 km northwest of the city center.  
653 Motorbikes are the main forms of transportation downtown and the primary source of mobile-  
654 based PM<sub>2.5</sub> (Vu Van et al., 2013). In Hanoi, the PM<sub>2.5</sub> Zn:Al ratio was 3.7, also the highest of  
655 any SPARTAN site, indicative of significant traffic and tire wear.

656  
657 *Hanoi Comparison:* SPARTAN PM<sub>2.5</sub> composition is generally consistent with Cohen et  
658 al.(2010). Slight differences are perhaps related to differences in sampling season and  
659 location. SPARTAN sea salt fraction was larger (2.5% vs. 0.6%), but with a lower ASO<sub>4</sub>  
660 fraction (17%) compared with Cohen et al. (2010) (29%). Sulfate tends to be lower in the  
661 spring-summer seasons, coinciding with our measurement period, which may explain the  
662 discrepancy. SPARTAN EBC (10%) is close to the Cohen et al. (2010) value of 8%, whereas  
663 SPARTAN RM (51%) and CM (16%) masses are slightly higher.

664  
665 **5.3.13 Pretoria, South Africa (n = 5)**

666 Pretoria is a high-altitude city (1300 m) surrounded by arid, low-intensity agriculture and  
667 extensive grasslands. The SPARTAN sampler is located on a 10m CSIR building rooftop 12 km  
668 east of downtown area (*pop.* 700,000). Preliminary measurements of south-hemisphere  
669 springtime show absolute PM<sub>2.5</sub> concentrations to be low, at 6.4  $\mu\text{g m}^{-3}$ . There are significant  
670 fractions of CM (22%) and EBC (22%), and low RM (14%). The PM<sub>2.5</sub> Zn:Al ratio (0.69)  
671 indicates vehicle traffic contributes to CM.

672 **6. Refining estimates of dry hourly PM<sub>2.5</sub> using  $\kappa_v$**

673 Our assessment of PM<sub>2.5</sub> hygroscopicity is determined by site-specific chemical composition. We  
674 then use the time-varying hygroscopicity to refine the PM<sub>2.5</sub> values inferred from nephelometer  
675 scatter.

676 **6.1. Relating PM<sub>2.5</sub> composition to  $\kappa_v$**

677 The outer pie charts of Figure 2 show the site-mean hygroscopic growth constant  $\kappa_v$ ,  
678 surrounded by the water contributions at 35% RH. The major contributors to PBW are ASO<sub>4</sub>,  
679 ANO<sub>3</sub>, RM, and sea salt, as inferred from the values listed in Table 2 and weighted by  
680 composition as in Eq. 5. ASO<sub>4</sub> and RM contribute similarly to total aerosol water whereas ANO<sub>3</sub>  
681 contributes less to PM<sub>2.5</sub> hygroscopicity due to its smaller mass. The contribution of sea salt to  
682 hygroscopicity can be significant, and makes a dominant contribution in both Rehovot and  
683 Buenos Aires.

684  
685 The parameter  $\kappa_v$ , when averaged across all sites, is 0.20, matching the generic estimate  
686  $\kappa_{v,tot} = 0.2$  applied in the initial SPARTAN study (Snider et al., 2015). Recently Brock et al.  
687 (2016) estimate  $\kappa_v$  values between 0.15 and 0.25 for ambient aerosols with 50% organic  
688 composition at subsaturated humidity. The local SPARTAN value in Atlanta (0.17) is consistent  
689 the value of  $0.16 \pm 0.07$  by Padró et al. (2012) in Atlanta. We found significant long-term  
690 differences in  $\kappa_{v,tot}$  between cities, from 0.15 in Ilorin to 0.28 in Rehovot, and differences  
691 between filters at single sites ( $\sigma \sim 0.05$ ). There is little correlation of  $\kappa_{v,tot}$  with changes in mass  
692 ( $r^2 < 0.01$ ). However, there are significant changes in  $\kappa_{v,tot}$  due to seasonality and specific



693 events (e.g. dust storms, fires). In Beijing, aerosol hygroscopicity was 50% higher in mid  
694 summer (August) due to increased sulfate, and in late winter (March) due to a relative increase in  
695 sea salt. A summertime sulfate peak also agrees with observations by Yang et al. (2011). Table 3  
696 shows the site-specific PBW in  $PM_{2.5}$ . At RH =35%, PBW ranges from 0.6 – 6  $\mu\text{g m}^{-3}$ ,  
697 comparable in absolute values to EBC. Above 80% RH PBW will account for more than half of  
698 aerosol mass. Accounting for this water component in nephelometer scatter motivates the  
699 following section.

## 700 6.2. Relating nephelometer scatter to dry (RH=35%) $PM_{2.5}$

701 We apply a temporally resolved, site-specific  $\kappa_v$  to refine our relationship between total  
702 nephelometer scatter and  $PM_{2.5}$ . We calculate a 45-day running mean aerosol volume-weighted  
703  $\kappa_v$  at each SPARTAN site. We then use the hygroscopic growth factors to estimate dry hourly  
704  $PM_{2.5}$  from hourly nephelometer measurements of ambient scatter and hourly measured RH.  
705 Appendix A2 describes the procedure in more detail.

706  
707 We compared our hourly  $PM_{2.5}$  in Beijing with  $PM_{2.5}$  measurements from a Beta Attenuation  
708 Monitor (MetOne) at the US Embassy, located 15 km away. The left panel of Figure 4 shows the  
709 time series of hourly dry  $PM_{2.5}$  concentrations predicted by SPARTAN during the summer.  
710 Pronounced temporal variation is apparent, with  $PM_{2.5}$  concentrations varying by more than an  
711 order of magnitude. A high degree of consistency is found with the BAM ( $r^2 = 0.67$ ). The  
712 exclusion of water uptake in hourly  $PM_{2.5}$  estimates (by setting all  $\kappa_v = 0$ ) decreased hourly  
713 correlations slightly to  $r^2 = 0.62$ . The average humidity in Beijing was 47% for the measurement  
714 period, corresponding to a mean 17% volume contribution by water ( $\kappa_v = 0.19$ ). Hygroscopic  
715 growth should play a more significant role under more humid conditions (e.g. Manila and  
716 Dhaka).

717  
718 The right panel shows daily-averaged  $PM_{2.5}$  ( $n = 148$ ). In 2014 there were 3167  
719 coincidentally available hours with which to compare. The coefficient of variation for averaged  
720 24-hour measurements remained high ( $r^2 = 0.70$ ). There was a mean offset of 10  $\mu\text{g m}^{-3}$ .  
721 However the slope is near unity (0.98), suggesting excellent proportionality between our  
722 nephelometer and the BAM instrument for  $PM_{2.5}$  concentrations below 200  $\mu\text{g m}^{-3}$ . Above this  
723 concentration, nephelometer signals become non-linear. The agreement remained similar for  
724 hourly values ( $r^2 = 0.67$ ).

## 726 7. Conclusions

727  
728 We have established a multi-country network where continuous monitoring with a 3-  
729 wavelength nephelometer is combined with a single multi-day composite filter sample to provide  
730 information on  $PM_{2.5}$ . Long-term average aerosol composition is inferred from the filters,  
731 including equivalent black carbon, sea salt, crustal material, ammoniated sulfate, and ammonium  
732 nitrate. This composition information was applied to calculate aerosol hygroscopicity, and in turn  
733 the relation between aerosol scatter at ambient and controlled RH. These data provide a  
734 consistent set of compositional measurements from 13 sites in 11 countries.

735

736 We report ongoing measurements of fine particulate matter (PM<sub>2.5</sub>), including compositional  
737 information, in 13 locations in two month or greater intervals all within a three-year span (2013-  
738 2016). The mean composition averaged for all SPARTAN sites is ammoniated sulfate (20% ±  
739 11%), crustal material (13.4% ± 9.9%), black carbon (11.9% ± 8.4%), ammonium nitrate (4.7%  
740 ± 3.0%), sea salt (2.3% ± 1.6%), trace element oxides (1.0% ± 1.1%), water (7.2% ± 3.3%) at  
741 35% RH, and residual matter, which is probably primarily organic (40% ± 24%).  
742

743 Analysis of filter samples reveals that several PM<sub>2.5</sub> chemical components varied by more  
744 than an order of magnitude between sites. Ammoniated sulfate ranged from 1 µg m<sup>-3</sup> in Buenos  
745 Aires to 17 µg m<sup>-3</sup> in Kanpur (dry season). Ammonium nitrate ranged from 0.2 µg m<sup>-3</sup>  
746 (Mammoth Cave, summertime) to 6.8 µg m<sup>-3</sup> (Kanpur, dry season). Equivalent black carbon  
747 ranged from 0.7 µg m<sup>-3</sup> (Mammoth Cave) to 8 µg m<sup>-3</sup> (Dhaka and Kanpur). Locations with  
748 enhanced sulfate tend to have enhancements in other PM components. For example, ammoniated  
749 sulfate and residual matter (probably organic) are highly correlated across sites ( $r^2 = 0.92$ ).  
750

751 Crustal material concentrations ranged from 1 µg m<sup>-3</sup> (Atlanta) to 16 µg m<sup>-3</sup> (Beijing).  
752 Measuring Zn:Al ratios in PM<sub>2.5</sub> was an effective way to determine anthropogenic contribution  
753 to crustal material. Ratios larger than 0.5 identified sites with significant road dust contributions  
754 (e.g. in Hanoi, Dhaka, Manila, and Kanpur). Some locations, such as Beijing and Buenos Aires,  
755 had both high anthropogenic and natural crustal material. Low coarse Zn:Al ratios were apparent  
756 during natural dust storms. Anthropogenic crustal material is an aerosol component neglected by  
757 most global models and which may deserve more attention.  
758

759 Potassium is a known marker for wood smoke. Enhanced K<sup>+</sup>:Al ratios were found in  
760 Singapore downwind of Indonesian forest fires, in Kanpur during the winter dry season from  
761 agricultural burning, and in Rehovot during a bonfire festival. Furthermore, these ratios were  
762 correlated with RM concentrations ( $r^2 = 0.73$ ), supporting the attribution of RM as mostly  
763 organic.  
764

765 SPARTAN measurements generally agree well with previous collocated studies. SPARTAN  
766 sulfate fractions are within 4% of fractions measured at eight of the ten collocated, though  
767 temporally non-coincident, studies. Dedicated contemporaneous collocation with IMPROVE at  
768 Mammoth Cave yielded a high degree of consistency with daily sulfate ( $r^2 = 0.86$ , slope = 1.03),  
769 daily PM<sub>2.5</sub> ( $r^2 = 0.76$ , slope = 1.12), and mean fractions for all major PM<sub>2.5</sub> components (within  
770 2%). Crustal material is typically consistent with the previous measurements, at 5-15%  
771 composition. SPARTAN equivalent black carbon ranged broadly, from 3% (Singapore) to 25%  
772 (Manila), and matched within a few percent of most previous works. Ammonium nitrate (4%)  
773 generally matched other sites, though it was sometimes lower, as in Beijing and Atlanta. Sea-salt  
774 was consistently low, as found in previous measurements. Sea salt fractions were highest in  
775 Buenos Aires and Rehovot (6%), reflecting natural coastal aerosols. SPARTAN residual matter  
776 is consistent with the combined organic and unknown masses. Comparing with collocated  
777 measurements supports the expectation that most of the RM is partially organic. Residual matter  
778 could also include unaccounted-for particle bound water, measurement error, and possibly  
779 unmeasured inorganic materials.  
780

781 We calculated the hygroscopic constant  $\kappa_v$  for individual PM<sub>2.5</sub> filters to estimate water at  
782 variable humidity, and to infer wet and water-free residual matter. Based on a range of literature,  
783 we treated residual matter as mostly organic, with constant  $\kappa_{v, RM} = 0.1$ . Residual matter and  
784 ammoniated sulfate largely determined overall water uptake in aerosols. These individual  
785 species, along with sea salt and ammonium nitrate, resulted in a mean mixed hygroscopic  
786 constant of 0.20, implying that for many sites, water content above 80% RH will account for  
787 more than half of aerosol mass. For cleanroom conditions of low humidity (35% RH), mean  
788 water composition was estimated to be 7% by mass.

789  
790 Water retention calculations allow for volumetric fluctuation estimates of aerosol water at  
791 variable RH. We subtracted the water component to predict dry nephelometer scatter as a  
792 function of time, anchored to filter masses at 35% RH. For Beijing, we assessed the consistency  
793 of SPARTAN predictions of hourly PM<sub>2.5</sub> values with BAM measurements taken 15 km away,  
794 and found temporal consistency ( $r^2 = 0.67$ ), with a slope near unity (0.98). The explained  
795 variance decreased to  $r^2 = 0.62$  when setting  $\kappa_v = 0$ . This comparison tested both SPARTAN  
796 instrumentation and our treatment of aerosol water uptake.

797  
798 These measurements provide chemical and physical data for future research on PM<sub>2.5</sub>.  
799 Collocation with sun photometer measurements of AOD connects satellite observations to  
800 ground-based measurements and provides information needed to evaluate chemical transport  
801 model simulations of the PM<sub>2.5</sub> to AOD ratio. As sampling expands, SPARTAN will provide  
802 long-term data on fine aerosol variability from around the world. Ongoing work includes an  
803 analysis of trace metal concentrations and interpreting SPARTAN measurements with a  
804 chemical transport model. The data are freely available as a public good at [www.spartan-](http://www.spartan-network.org)  
805 [network.org](http://www.spartan-network.org). We welcome expressions of interest to join this grass-roots network.

## 806 **Acknowledgements**

807  
808 SPARTAN is an IGAC-endorsed activity ([www.igacproject.org](http://www.igacproject.org)). The Natural Sciences and  
809 Engineering Research Council (NSERC) of Canada supported this work. We are grateful to  
810 many who have offered helpful comments and advice on the creation of this network including  
811 Jay Al-Saadi, Ross Anderson, Kalpana Balakrishnan, Len Barrie, Sundar Christopher, Matthew  
812 Cooper, Jim Crawford, Doug Dockery, Jill Engel-Cox, Greg Evans, Markus Fiebig, Allan  
813 Goldstein, Judy Guernsey, Ray Hoff, Rudy Husar, Mike Jerrett, Michaela Kendall, Rich  
814 Kleidman, Petros Koutrakis, Glynis Lough, Doreen Neil, John Ogren, Norm O'Neil, Jeff Pierce,  
815 Thomas Holzer-Popp, Ana Prados, Lorraine Remer, Sylvia Richardson, and Frank Speizer. Data  
816 collection Rehovot was supported in part by the Environmental Health Fund (Israel) and the  
817 Weizmann Institute. Partial support for the ITB site was under the grant HIBAH WCU-ITB. The  
818 site at IIT Kanpur is supported in part by National Academy of Sciences and USAID. The views  
819 expressed here are of authors and do not necessarily reflect those of NAS or USAID. The  
820 Singapore site is supported by the Singapore National Research Foundation (NRF) through the  
821 Singapore-MIT Alliance for Research and Technology (SMART), Center for Environmental  
822 Sensing and Modeling.

823



## 824 8. References

- 825  
826 Ahmed, S.: Food and Agriculture in Bangladesh, *Encycl. Food Agric. Ethics*, doi:10.1007/978-94-007-6167-4\_61-2,  
827 2013.
- 828 Asa-Awuku, A., Moore, R. H., Nenes, A., Bahreini, R., Holloway, J. S., Brock, C. A., Middlebrook, A. M.,  
829 Ryerson, T. B., Jimenez, J. L., DeCarlo, P. F., Hecobian, A., Weber, R. J., Stickel, R., Tanner, D. J., and Huey, L.  
830 G.: Airborne cloud condensation nuclei measurements during the 2006 Texas Air Quality Study, *J. Geophys. Res.*  
831 *Atmos.*, 116(D11), D11201, doi:10.1029/2010JD014874, 2011.
- 832 Badger, C. L., George, I., Griffiths, P. T., Braban, C. F., Cox, R. A., and Abbatt, J. P. D.: Phase transitions and  
833 hygroscopic growth of aerosol particles containing humic acid and mixtures of humic acid and ammonium sulphate,  
834 *Atmos. Chem. Phys.*, 6(3), 755–768, doi:10.5194/acp-6-755-2006, 2006.
- 835 Barnard, J. C., Volkamer, R., and Kassianov, E. I.: Estimation of the mass absorption cross section of the organic  
836 carbon component of aerosols in the Mexico City Metropolitan Area, *Atmos. Chem. Phys.*, 8(22), 6665–6679,  
837 doi:10.5194/acp-8-6665-2008, 2008.
- 838 Begum, B. A., Biswas, S. K., Markwitz, A., and Hopke, P. K.: Identification of sources of fine and coarse particulate  
839 matter in Dhaka, Bangladesh, *Aerosol Air Qual. Res.*, 10, 345–353, doi:10.4209/aaqr.2009.12.0082, 2010.
- 840 Begum, B. A., Hossain, A., Nahar, N., Markwitz, A., and Hopke, P. K.: Organic and Black Carbon in PM<sub>2.5</sub> at an  
841 Urban Site at Dhaka, Bangladesh, *Aerosol Air Qual. Res.*, 12(6), 1062–1072, 2012.
- 842 Behera, S. N., and Sharma, M.: Reconstructing Primary and Secondary Components of PM<sub>2.5</sub> Composition for an  
843 Urban Atmosphere, *Aerosol Sci. Technol.*, 44(11), 983–992, doi:10.1080/02786826.2010.504245, 2010.
- 844 Bell, M. L., Dominici, F., Ebisu, K., Zeger, S. L., and Samet, J. M.: Spatial and Temporal Variation in PM<sub>2.5</sub>  
845 Chemical Composition in the United States for Health Effects Studies, *Environ. Health Perspect.*, 115(7), 989–995,  
846 doi:10.2307/4619499, 2007.
- 847 Bezantakos, S., Barmounis, K., Giamarelou, M., Bossioli, E., Tombrou, M., Mihalopoulos, N., Eleftheriadis, K.,  
848 Kalogiros, J., D. Allan, J., Bacak, A., Percival, C. J., Coe, H., and Biskos, G.: Chemical composition and  
849 hygroscopic properties of aerosol particles over the Aegean Sea, *Atmos. Chem. Phys.*, 13(22), 11595–11608,  
850 doi:10.5194/acp-13-11595-2013, 2013.
- 851 Bond, T. C. and Bergstrom, R. W.: Light Absorption by Carbonaceous Particles: An Investigative Review, *Aerosol*  
852 *Sci. Technol.*, 40(1), 27–67, doi:10.1080/02786820500421521, 2006.
- 853 Boys, B. L., Martin, R. V., van Donkelaar, A., MacDonell, R. J., Hsu, N. C., Cooper, M. J., Yantosca, R. M., Lu, Z.,  
854 Streets, D. G., Zhang, Q., and Wang, S. W.: Fifteen-Year Global Time Series of Satellite-Derived Fine Particulate  
855 Matter, *Environ. Sci. Technol.*, 48(19), 11109–11118, doi:10.1021/es502113p, 2014.
- 856 Brauer, M., Freedman, G., Frostad, J., van Donkelaar, A., Martin, R. V., Dentener, F., Dingenen, R. van, Estep, K.,  
857 Amini, H., Apte, J. S., Balakrishnan, K., Barregard, L., Broday, D., Feigin, V., Ghosh, S., Hopke, P. K., Knibbs, L.  
858 D., Kokubo, Y., Liu, Y., Ma, S., Morawska, L., Sangrador, J. L. T., Shaddick, G., Anderson, H. R., Vos, T.,  
859 Forouzanfar, M. H., Burnett, R. T., and Cohen, A.: Ambient Air Pollution Exposure Estimation for the Global  
860 Burden of Disease 2013, *Environ. Sci. Technol.*, doi:10.1021/acs.est.5b03709, 2015.
- 861 Brock, C. A., Wagner, N. L., Anderson, B. E., Attwood, A. R., Beyersdorf, A., Campuzano-Jost, P., Carlton, A. G.,  
862 Day, D. A., Diskin, G. S., Gordon, T. D., Jimenez, J. L., Lack, D. A., Liao, J., Markovic, M. Z., Middlebrook, A.  
863 M., Ng, N. L., Perring, A. E., Richardson, M. S., Schwarz, J. P., Washenfelder, R. A., Welti, A., Xu, L., Ziemba, L.  
864 D., and Murphy, D. M.: Aerosol optical properties in the southeastern United States in summer – Part 1:  
865 Hygroscopic growth, *Atmos. Chem. Phys.*, 16(8), 4987–5007, doi:10.5194/acp-16-4987-2016, 2016.
- 866 Butler, A. J., Andrew, M. S., and Russell, A. G.: Daily sampling of PM<sub>2.5</sub> in Atlanta: Results of the first year of the  
867 Assessment of Spatial Aerosol Composition in Atlanta study, *J. Geophys. Res. Atmos.*, 108(D7), 8415,  
868 doi:10.1029/2002JD002234, 2003.
- 869 Canagaratna, M. R., Jimenez, J. L., Kroll, J. H., Chen, Q., Kessler, S. H., Massoli, P., Hildebrandt Ruiz, L., Fortner,  
870 E., Williams, L. R., Wilson, K. R., Surratt, J. D., Donahue, N. M., Jayne, J. T., and Worsnop, D. R.: Elemental ratio

871 measurements of organic compounds using aerosol mass spectrometry: characterization, improved calibration, and  
872 implications, *Atmos. Chem. Phys.*, 15(1), 253–272, doi:10.5194/acp-15-253-2015, 2015.

873 Carrico, C. M., Petters, M. D., Kreidenweis, S. M., Sullivan, A. P., McMeeking, G. R., Levin, E. J. T., Engling, G.,  
874 Malm, W. C., and Collett, J. L.: Water uptake and chemical composition of fresh aerosols generated in open burning  
875 of biomass, *Atmos. Chem. Phys.*, 10(11), 5165–5178, doi:10.5194/acp-10-5165-2010, 2010.

876 Chakraborty, A., Bhattu, D., Gupta, T., Tripathi, S. N., and Canagaratna, M. R.: Real-time measurements of ambient  
877 aerosols in a polluted Indian city: Sources, characteristics, and processing of organic aerosols during foggy and  
878 nonfoggy periods, *J. Geophys. Res. Atmos.*, 120(17), 2015JD023419, doi:10.1002/2015JD023419, 2015.

879 Chang, R. Y.-W., Slowik, J. G., Shantz, N. C., Vlasenko, A., Liggio, J., Sjostedt, S. J., Leaitch, W. R., and Abbatt, J.  
880 P. D.: The hygroscopicity parameter ( $\kappa$ ) of ambient organic aerosol at a field site subject to biogenic and  
881 anthropogenic influences: relationship to degree of aerosol oxidation, *Atmos. Chem. Phys.*, 10(11), 5047–5064,  
882 doi:10.5194/acp-10-5047-2010, 2010.

883 Chen, H., Goldberg, M. S., and Villeneuve, P. J.: A systematic review of the relation between long-term exposure to  
884 ambient air pollution and chronic diseases., *Rev. Environ. Health*, 23(4), 243–297, 2008.

885 Chen, Z., Wang, J.-N., Ma, G.-X., and Zhang, Y.-S.: China tackles the health effects of air pollution, *Lancet*,  
886 382(9909), 1959–1960, 2013.

887 Chow, J. C., Watson, J. G., Park, K., Lowenthal, D. H., Robinson, N. F., and Magliano, K. A.: Comparison of  
888 particle light scattering and fine particulate matter mass in central California., *J. Air Waste Manage. Assoc.*, 56(4),  
889 398–410, 2006.

890 Chu, S.-H.: PM<sub>2.5</sub> episodes as observed in the speciation trends network, *Atmos. Environ.*, 38(31), 5237–5246,  
891 doi:10.1016/j.atmosenv.2004.01.055, 2004.

892 Clarisse, L., Clerbaux, C., Dentener, F., Hurtmans, D., and Coheur, P.-F.: Global ammonia distribution derived from  
893 infrared satellite observations, *Nat. Geosci.*, 2(7), 479–483, 2009.

894 Cohen, D. D., Garton, D., Stelcer, E., Wang, T., Poon, S., Kim, J., Oh, S. N., Shin, H.-J., Ko, M. Y., and Santos, F.:  
895 Characterisation of PM<sub>2.5</sub> and PM<sub>10</sub> fine particle pollution in several Asian regions., 2002.

896 Cohen, D. D., Stelcer, E., Santos, F. L., Prior, M., Thompson, C., and Pabroa, P. C. B.: Fingerprinting and source  
897 apportionment of fine particle pollution in Manila by IBA and PMF techniques: A 7-year study, *X-Ray Spectrom.*,  
898 38(1), 18–25, doi:10.1002/xrs.1112, 2009.

899 Cohen, D. D., Crawford, J., Stelcer, E., and Bac, V. T.: Characterisation and source apportionment of fine  
900 particulate sources at Hanoi from 2001 to 2008, *Atmos. Environ.*, 44(3), 320–328,  
901 doi:10.1016/j.atmosenv.2009.10.037, 2010.

902 Councill, T. B., Duckenfield, K. U., Landa, E. R., and Callender, E.: Tire-Wear Particles as a Source of Zinc to the  
903 Environment, *Environ. Sci. Technol.*, 38(15), 4206–4214, doi:10.1021/es034631f, 2004.

904 Dabek-Zlotorzynska, E., Dann, T. F., Kalyani Martinelango, P., Celo, V., Brook, J. R., Mathieu, D., Ding, L., and  
905 Austin, C. C.: Canadian National Air Pollution Surveillance (NAPS) PM<sub>2.5</sub> speciation program: Methodology and  
906 PM<sub>2.5</sub> chemical composition for the years 2003–2008, *Atmos. Environ.*, 45(3), 673–686, 2011.

907 van Donkelaar, A., Martin, R. V., Brauer, M., and Boys, B. L.: Use of Satellite Observations for Long-Term  
908 Exposure Assessment of Global Concentrations of Fine Particulate Matter, *Environ. Health Perspect.*, 123(2), 135–  
909 143, doi:10.1289/ehp.1408646, 2015.

910 Duplissy, J., DeCarlo, P. F., Dommen, J., Alfarra, M. R., Metzger, A., Barmapadimos, I., Prevot, A. S. H.,  
911 Weingartner, E., Tritscher, T., Gysel, M., Aiken, A. C., Jimenez, J. L., Canagaratna, M. R., Worsnop, D. R., Collins,  
912 D. R., Tomlinson, J., and Baltensperger, U.: Relating hygroscopicity and composition of organic aerosol particulate  
913 matter, *Atmos. Chem. Phys.*, 11(3), 1155–1165, doi:10.5194/acp-11-1155-2011, 2011.

914 Dusek, U., Frank, G. P., Massling, A., Zeromskiene, K., Iinuma, Y., Schmid, O., Helas, G., Hennig, T.,  
915 Wiedensohler, A., and Andreae, M. O.: Water uptake by biomass burning aerosol at sub- and supersaturated  
916 conditions: closure studies and implications for the role of organics, *Atmos. Chem. Phys.*, 11(18), 9519–9532,

- 917 doi:10.5194/acp-11-9519-2011, 2011.
- 918 Falkovich, A. H., Schkolnik, G., Ganor, E., and Rudich, Y.: Adsorption of organic compounds pertinent to urban  
919 environments onto mineral dust particles, *J. Geophys. Res. Atmos.*, 109(D2), n/a–n/a, doi:10.1029/2003JD003919,  
920 2004.
- 921 Fang, T., Guo, H., Verma, V., Peltier, R. E., and Weber, R. J.: PM<sub>2.5</sub> water-soluble elements in the southeastern  
922 United States: automated analytical method development, spatiotemporal distributions, source apportionment, and  
923 implications for health studies, *Atmos. Chem. Phys.*, 15(20), 11667–11682, doi:10.5194/acp-15-11667-2015, 2015.
- 924 Forouzanfar, M. H., Alexander, L., Anderson, H. R., Bachman, V. F., Biryukov, S., Brauer, M., Burnett, R., Casey,  
925 D., Coates, M. M., Cohen, A., Delwiche, K., Estep, K., Frostad, J. J., KC, A., Kyu, H. H., Moradi-Lakeh, M., Ng,  
926 M., Slepak, E. L., Thomas, B. A., Wagner, J., Aasvang, G. M., Abbafati, C., Ozgoren, A. A., Abd-Allah, F., Abera,  
927 S. F., Aboyans, V., Abraham, B., Abraham, J. P., Abubakar, I., Abu-Rmeileh, N. M. E., Aburto, T. C., Achoki, T.,  
928 Adelekan, A., Adofo, K., Adou, A. K., Adsuar, J. C., Afshin, A., Agardh, E. E., Al Khabouri, M. J., Al Lami, F. H.,  
929 Alam, S. S., Alasfoor, D., Albittar, M. I., Alegretti, M. A., Aleman, A. V., Alemu, Z. A., Alfonso-Cristancho, R.,  
930 Alhabib, S., Ali, R., Ali, M. K., Alla, F., Allebeck, P., Allen, P. J., Alsharif, U., Alvarez, E., Alvis-Guzman, N.,  
931 Amankwaa, A. A., Amare, A. T., Ameh, E. A., Ameli, O., Amini, H., Ammar, W., Anderson, B. O., Antonio, C. A.  
932 T., Anwari, P., Cunningham, S. A., Arnlöv, J., Arsenijevic, V. S. A., Artaman, A., Asghar, R. J., Assadi, R., Atkins,  
933 L. S., Atkinson, C., Avila, M. A., Awuah, B., Badawi, A., Bahit, M. C., Bakfalouni, T., Balakrishnan, K., Balalla,  
934 S., Balu, R. K., Banerjee, A., Barber, R. M., Barker-Collo, S. L., Barquera, S., Barregard, L., Barrero, L. H.,  
935 Barrientos-Gutierrez, T., Basto-Abreu, A. C., Basu, A., Basu, S., Basulaiman, M. O., Ruvalcaba, C. B., Beardsley,  
936 J., Bedi, N., Bekele, T., Bell, M. L., Benjet, C., Bennett, D. A., et al.: Global, regional, and national comparative risk  
937 assessment of 79 behavioural, environmental and occupational, and metabolic risks or clusters of risks in 188  
938 countries, 1990–2013: a systematic analysis for the Global Burden of Disease Study 2013, *Lancet*,  
939 doi:10.1016/S0140-6736(15)00128-2, 2015.
- 940 Fountoukis, C. and Nenes, A.: ISORROPIA II: a computationally efficient thermodynamic equilibrium model for  
941 aerosols, *Atmos. Chem. Phys.*, 7(17), 4639–4659, doi:10.5194/acp-7-4639-2007, 2007.
- 942 Fujii, Y., Iriana, W., Oda, M., Puriwigati, A., Tohno, S., Lestari, P., Mizohata, A., and Huboyo, H. S.:  
943 Characteristics of carbonaceous aerosols emitted from peatland fire in Riau, Sumatra, Indonesia, *Atmos. Environ.*,  
944 87, 164–169, doi:10.1016/j.atmosenv.2014.01.037, 2014.
- 945 Generoso, S., Bréon, F.-M., Balkanski, Y., Boucher, O., and Schulz, M.: Improving the seasonal cycle and  
946 interannual variations of biomass burning aerosol sources, *Atmos. Chem. Phys.*, 3(4), 1211–1222, doi:10.5194/acp-  
947 3-1211-2003, 2003.
- 948 Gibson, M. D., Heal, M. R., Bache, D. H., Hursthouse, A. S., Beverland, I. J., Craig, S. E., Clark, C. F., Jackson, M.  
949 H., Guernsey, J. R., and Jones, C.: Using Mass Reconstruction along a Four-Site Transect as a Method to Interpret  
950 PM<sub>10</sub> in West-Central Scotland, United Kingdom, *J. Air Waste Manage. Assoc.*, 59(12), 1429–1436,  
951 doi:10.3155/1047-3289.59.12.1429, 2009.
- 952 Gibson, M. D., Pierce, J. R., Waugh, D., Kuchta, J. S., Chisholm, L., Duck, T. J., Hopper, J. T., Beauchamp, S.,  
953 King, G. H., Franklin, J. E., Leitch, W. R., Wheeler, A. J., Li, Z., Gagnon, G. A., and Palmer, P. I.: Identifying the  
954 sources driving observed PM<sub>2.5</sub> temporal variability over Halifax, Nova Scotia, during BORTAS-B, *Atmos. Chem.*  
955 *Phys.*, 13(14), 7199–7213, doi:10.5194/acp-13-7199-2013, 2013a.
- 956 Gibson, M. D., Heal, M. R., Li, Z., Kuchta, J., King, G. H., Hayes, A., and Lambert, S.: The spatial and seasonal  
957 variation of nitrogen dioxide and sulfur dioxide in Cape Breton Highlands National Park, Canada, and the  
958 association with lichen abundance, *Atmos. Environ.*, 64(0), 303–311,  
959 doi:http://dx.doi.org/10.1016/j.atmosenv.2012.09.068, 2013b.
- 960 Giordano, M. R., Short, D. Z., Hosseini, S., Lichtenberg, W., and Asa-Awuku, A. A.: Changes in Droplet Surface  
961 Tension Affect the Observed Hygroscopicity of Photochemically Aged Biomass Burning Aerosol, *Environ. Sci.*  
962 *Technol.*, 47(19), 10980–10986, doi:10.1021/es401867j, 2013.
- 963 Graham, B., Falkovich, A. H., Rudich, Y., Maenhaut, W., Guyon, P., and Andreae, M. O.: Local and regional  
964 contributions to the atmospheric aerosol over Tel Aviv, Israel: a case study using elemental, ionic and organic  
965 tracers, *Atmos. Environ.*, 38(11), 1593–1604, doi:http://dx.doi.org/10.1016/j.atmosenv.2003.12.015, 2004.

- 966 Hand, J. and Malm, W. C.: Review of the IMPROVE Equation for Estimating Ambient Light Extinction  
967 Coefficients, Colorado State University, Fort Collins., 2006.
- 968 Hand, J. L., Schichtel, B. A., Pitchford, M., Malm, W. C., and Frank, N. H.: Seasonal composition of remote and  
969 urban fine particulate matter in the United States, *J. Geophys. Res.*, 117(D5), D05209, doi:10.1029/2011JD017122,  
970 2012.
- 971 Henning, S., Weingartner, E., Schwikowski, M., Gäggeler, H. W., Gehrig, R., Hinz, K.-P., Trimborn, A., Spengler,  
972 B., and Baltensperger, U.: Seasonal variation of water-soluble ions of the aerosol at the high-alpine site Jungfraujoch  
973 (3580 m asl), *J. Geophys. Res. Atmos.*, 108(D1), 4030, doi:10.1029/2002JD002439, 2003.
- 974 Hersey, S. P., Craven, J. S., Metcalf, A. R., Lin, J., Latham, T., Suski, K. J., Cahill, J. F., Duong, H. T., Sorooshian,  
975 A., Jonsson, H. H., Shiraiwa, M., Zuend, A., Nenes, A., Prather, K. A., Flagan, R. C., and Seinfeld, J. H.:  
976 Composition and hygroscopicity of the Los Angeles Aerosol: CalNex, *J. Geophys. Res. Atmos.*, 118(7), 3016–3036,  
977 doi:10.1002/jgrd.50307, 2013.
- 978 Holben, B. N., Eck, T. F., Slutsker, I., Tanré, D., Buis, J. P., Setzer, A., Vermote, E., Reagan, J. A., Kaufman, Y. J.,  
979 Nakajima, T., Lavenu, F., Jankowiak, I., and Smirnov, A.: AERONET—A Federated Instrument Network and Data  
980 Archive for Aerosol Characterization, *Remote Sens. Environ.*, 66(1), 1–16, doi:http://dx.doi.org/10.1016/S0034-  
981 4257(98)00031-5, 1998.
- 982 Huang, J. P., Liu, J. J., Chen, B., and Nasiri, S. L.: Detection of anthropogenic dust using CALIPSO lidar  
983 measurements, *Atmos. Chem. Phys.*, 15(20), 11653–11665, doi:10.5194/acp-15-11653-2015, 2015.
- 984 IMPROVE: Reconstructing Light Extinction from Aerosol Measurements, *Reconstr. Light Extinction from Aerosol*  
985 *Meas. Interag. Monit. Prot. Vis. Environ.* [online] Available from:  
986 <http://views.cira.colostate.edu/fed/DataWizard/Default.aspx> (Accessed 20 May 2012), 2015.
- 987 IPCC: Climate Change 2013: The Physical Science Basis. Contribution of Working Group I to the Fifth Assessment  
988 Report of the Intergovernmental Panel on Climate Change, 5th ed., edited by T. F. Stocker, D. Qin, G.-K. Plattner,  
989 M. Tignor, S. K. Allen, J. Boschung, A. Nauels, Y. Xia, V. Bex, and P. M. Midgley, Cambridge University Press,  
990 Cambridge, United Kingdom and New York, NY, USA., 2013.
- 991 Jasan, R. C., Plá, R. R., Invernizzi, R., and Dos Santos, M.: Characterization of atmospheric aerosol in Buenos  
992 Aires, Argentina, *J. Radioanal. Nucl. Chem.*, 281(1), 101–105, doi:10.1007/s10967-009-0071-1, 2009.
- 993 Jimenez, J. L., Canagaratna, M. R., Donahue, N. M., Prevot, A. S. H., Zhang, Q., Kroll, J. H., DeCarlo, P. F., Allan,  
994 J. D., Coe, H., Ng, N. L., Aiken, A. C., Docherty, K. S., Ulbrich, I. M., Grieshop, A. P., Robinson, A. L., Duplissy,  
995 J., Smith, J. D., Wilson, K. R., Lanz, V. A., Hueglin, C., Sun, Y. L., Tian, J., Laaksonen, A., Raatikainen, T.,  
996 Rautiainen, J., Vaattovaara, P., Ehn, M., Kulmala, M., Tomlinson, J. M., Collins, D. R., Cubison, M. J., E., Dunlea,  
997 J., Huffman, J. A., Onasch, T. B., Alfarra, M. R., Williams, P. I., Bower, K., Kondo, Y., Schneider, J., Drewnick, F.,  
998 Borrmann, S., Weimer, S., Demerjian, K., Salcedo, D., Cottrell, L., Griffin, R., Takami, A., Miyoshi, T.,  
999 Hatakeyama, S., Shimojo, A., Sun, J. Y., Zhang, Y. M., Dzepina, K., Kimmel, J. R., Sueper, D., Jayne, J. T.,  
1000 Herndon, S. C., Trimborn, A. M., Williams, L. R., Wood, E. C., Middlebrook, A. M., Kolb, C. E., Baltensperger, U.,  
1001 and Worsnop, D. R.: Evolution of Organic Aerosols in the Atmosphere, *Sci.*, 326 (5959), 1525–1529,  
1002 doi:10.1126/science.1180353, 2009.
- 1003 Kahn, R. A. and Gaitley, B. J.: An analysis of global aerosol type as retrieved by MISR, *J. Geophys. Res. Atmos.*,  
1004 120(9), 4248–4281, doi:10.1002/2015JD023322, 2015.
- 1005 Kloog, I., Koutrakis, P., Coull, B. A., Lee, H. J., and Schwartz, J.: Assessing temporally and spatially resolved  
1006 PM<sub>2.5</sub> exposures for epidemiological studies using satellite aerosol optical depth measurements, *Atmos. Environ.*,  
1007 45(35), 6267–6275, doi:10.1016/j.atmosenv.2011.08.066, 2011.
- 1008 Kloog, I., Ridgway, B., Koutrakis, P., Coull, B. A., and Schwartz, J. D.: Long- and Short-Term Exposure to PM(2.5)  
1009 and Mortality: Using Novel Exposure Models, *Epidemiology*, 24(4), 555–561,  
1010 doi:10.1097/EDE.0b013e318294beaa, 2013.
- 1011 Koepke, P., Hess, M., Schult, I., and Shettle, E. P.: Global Aerosol Dataset, Report N 243, Hamburg., 1997.
- 1012 Kreidenweis, S. M., Petters, M. D., and DeMott, P. J.: Single-parameter estimates of aerosol water content, *Environ.*

- 1013 Res. Lett., 3(3), 35002, doi:10.1088/1748-9326/3/3/035002, 2008.
- 1014 Laden, F., Schwartz, J., Speizer, F. E., and Dockery, D. W.: Reduction in Fine Particulate Air Pollution and  
1015 Mortality, *Am. J. Respir. Crit. Care Med.*, 173(6), 667–672, doi:10.1164/rccm.200503-443OC, 2006.
- 1016 Latham, J., Cumani, R., Rosati, I., and Bloise, M.: Global Land Cover SHARE (GLC-SHARE) database Beta-  
1017 Release Version 1.0-2014, Rome., 2014.
- 1018 Latham, T. L., Beyersdorf, A. J., Thornhill, K. L., Winstead, E. L., Cubison, M. J., Hecobian, A., Jimenez, J. L.,  
1019 Weber, R. J., Anderson, B. E., and Nenes, A.: Analysis of CCN activity of Arctic aerosol and Canadian biomass  
1020 burning during summer 2008, *Atmos. Chem. Phys.*, 13(5), 2735–2756, doi:10.5194/acp-13-2735-2013, 2013.
- 1021 Lee, H. J., Coull, B. A., Bell, M. L., and Koutrakis, P.: Use of satellite-based aerosol optical depth and spatial  
1022 clustering to predict ambient PM<sub>2.5</sub> concentrations., *Environ. Res.*, 118, 8–15, doi:10.1016/j.envres.2012.06.011,  
1023 2012.
- 1024 Lelieveld, J., Evans, J. S., Fnais, M., Giannadaki, D., and Pozzer, A.: The contribution of outdoor air pollution  
1025 sources to premature mortality on a global scale, *Nature*, 525(7569), 367–371, 2015.
- 1026 Lepeule, J., Laden, F., Dockery, D., and Schwartz, J.: Chronic Exposure to Fine Particles and Mortality: An  
1027 Extended Follow-up of the Harvard Six Cities Study from 1974 to 2009, *Environ. Health Perspect.*, 120(7), 965–  
1028 970, doi:10.1289/ehp.1104660, 2012.
- 1029 Lestari, P., and Mauliadi, Y. D.: Source apportionment of particulate matter at urban mixed site in Indonesia using  
1030 PMF, *Atmos. Environ.*, 43(10), 1760–1770, doi:http://dx.doi.org/10.1016/j.atmosenv.2008.12.044, 2009.
- 1031 Lin, C., Li, Y., Yuan, Z., Lau, A. K. H., Li, C., and Fung, J. C. H.: Using satellite remote sensing data to estimate the  
1032 high-resolution distribution of ground-level PM<sub>2.5</sub>, *Remote Sens. Environ.*, 156, 117–128,  
1033 doi:10.1016/j.rse.2014.09.015, 2015.
- 1034 Lippmann, M.: Toxicological and epidemiological studies of cardiovascular effects of ambient air fine particulate  
1035 matter (PM<sub>2.5</sub>) and its chemical components: Coherence and public health implications, *Crit. Rev. Toxicol.*, 44(4),  
1036 299–347, doi:10.3109/10408444.2013.861796, 2014.
- 1037 Liu, Y., Monod, A., Tritscher, T., Praplan, A. P., DeCarlo, P. F., Temime-Roussel, B., Quivet, E., Marchand, N.,  
1038 Dommen, J., and Baltensperger, U.: Aqueous phase processing of secondary organic aerosol from isoprene  
1039 photooxidation, *Atmos. Chem. Phys.*, 12(13), 5879–5895, doi:10.5194/acp-12-5879-2012, 2012.
- 1040 Malm, W. C., Sisler, J. F., Huffman, D., Eldred, R. A., and Cahill, T. A.: Spatial and seasonal trends in particle  
1041 concentration and optical extinction in the United States, *J. Geophys. Res.*, 99(D1), 1347–1370, 1994.
- 1042 Misra, A., Gaur, A., Bhattu, D., Ghosh, S., Dwivedi, A. K., Dalai, R., Paul, D., Gupta, T., Tare, V., Mishra, S. K.,  
1043 Singh, S., and Tripathi, S. N.: An overview of the physico-chemical characteristics of dust at Kanpur in the central  
1044 Indo-Gangetic basin, *Atmos. Environ.*, 97, 386–396, doi:10.1016/j.atmosenv.2014.08.043, 2014.
- 1045 Munchak, L. A., Schichtel, B. A., Sullivan, A. P., Holden, A. S., Kreidenweis, S. M., Malm, W. C., and Collett, J.  
1046 L.: Development of wildland fire particulate smoke marker to organic carbon emission ratios for the conterminous  
1047 United States, *Atmos. Environ.*, 45(2), 395–403, doi:10.1016/j.atmosenv.2010.10.006, 2011.
- 1048 Oanh, N. T. K., Upadhyay, N., Zhuang, Y.-H., Hao, Z.-P., Murthy, D. V. S., Lestari, P., Villarin, J. T., Chengchua,  
1049 K., Co, H. X., Dung, N. T., and Lindgren, E. S.: Particulate air pollution in six Asian cities: Spatial and temporal  
1050 distributions, and associated sources, *Atmos. Environ.*, 40(18), 3367–3380,  
1051 doi:http://dx.doi.org/10.1016/j.atmosenv.2006.01.050, 2006.
- 1052 Padró, L. T., Moore, R. H., Zhang, X., Rastogi, N., Weber, R. J., and Nenes, A.: Mixing state and compositional  
1053 effects on CCN activity and droplet growth kinetics of size-resolved CCN in an urban environment, *Atmos. Chem.*  
1054 *Phys.*, 12(21), 10239–10255, doi:10.5194/acp-12-10239-2012, 2012.
- 1055 Patadia, F., Kahn, R. A., Limbacher, J. A., Burton, S. P., Ferrare, R. A., Hostetler, C. A., and Hair, J. W.: Aerosol  
1056 airmass type mapping over the Urban Mexico City region from space-based multi-angle imaging, *Atmos. Chem.*  
1057 *Phys.*, 13(18), 9525–9541, doi:10.5194/acp-13-9525-2013, 2013.
- 1058 Petters, M. D. and Kreidenweis, S. M.: A single parameter representation of hygroscopic growth and cloud

- 1059 condensation nucleus activity, *Atmos. Chem. Phys.*, 7(8), 1961–1971, doi:10.5194/acp-7-1961-2007, 2007.
- 1060 Petters, M. D. and Kreidenweis, S. M.: A single parameter representation of hygroscopic growth and cloud  
1061 condensation nucleus activity – Part 2: Including solubility, *Atmos. Chem. Phys.*, 8(20), 6273–6279,  
1062 doi:10.5194/acp-8-6273-2008, 2008.
- 1063 Petters, M. D. and Kreidenweis, S. M.: A single parameter representation of hygroscopic growth and cloud  
1064 condensation nucleus activity; Part 3: Including surfactant partitioning, *Atmos. Chem. Phys.*, 13(2), 1081–1091,  
1065 doi:10.5194/acp-13-1081-2013, 2013.
- 1066 Petzold, A., Ogren, J. A., Fiebig, M., Laj, P., Li, S.-M., Baltensperger, U., Holzer-Popp, T., Kinne, S., Pappalardo,  
1067 G., Sugimoto, N., Wehrli, C., Wiedensohler, A., and Zhang, X.-Y.: Recommendations for reporting “black carbon”  
1068 measurements, *Atmos. Chem. Phys.*, 13(16), 8365–8379, doi:10.5194/acp-13-8365-2013, 2013.
- 1069 Philip, S., Martin, R. V., van Donkelaar, A., Lo, J. W.-H., Wang, Y., Chen, D., Zhang, L., Kasibhatla, P. S., Wang,  
1070 S., Zhang, Q., Lu, Z., Streets, D. G., Bittman, S., and Macdonald, D. J.: Global Chemical Composition of Ambient  
1071 Fine Particulate Matter for Exposure Assessment, *Environ. Sci. Technol.*, 48(22), 13060–13068,  
1072 doi:10.1021/es502965b, 2014a.
- 1073 Philip, S., Martin, R. V., Pierce, J. R., Jimenez, J. L., Zhang, Q., Canagaratna, M. R., Spracklen, D. V., Nowlan, C.  
1074 R., Lamsal, L. N., Cooper, M. J., and Krotkov, N. A.: Spatially and seasonally resolved estimate of the ratio of  
1075 organic mass to organic carbon, *Atmos. Environ.*, 87, 34–40, doi:10.1016/j.atmosenv.2013.11.065, 2014b.
- 1076 Pitchford, M., Malm, W., Schichtel, B., Kumar, N., Lowenthal, D., and Hand, J.: Revised Algorithm for Estimating  
1077 Light Extinction from IMPROVE Particle Speciation Data, *J. Air Waste Manage. Assoc.*, 57(11), 1326–1336,  
1078 doi:10.3155/1047-3289.57.11.1326, 2007.
- 1079 Prenni, A. J., Petters, M. D., Kreidenweis, S. M., DeMott, P. J., and Ziemann, P. J.: Cloud droplet activation of  
1080 secondary organic aerosol, *J. Geophys. Res.*, 112(D10), D10223, doi:10.1029/2006JD007963, 2007.
- 1081 Putaud, J.-P., Raes, F., Van Dingenen, R., Brüggemann, E., Facchini, M.-C., Decesari, S., Fuzzi, S., Gehrig, R.,  
1082 Hüglin, C., Laj, P., Lorbeer, G., Maenhaut, W., Mihalopoulos, N., Müller, K., Querol, X., Rodriguez, S., Schneider,  
1083 J., Spindler, G., Brink, H. ten, Tørseth, K., and Wiedensohler, A.: A European aerosol phenomenology—2: chemical  
1084 characteristics of particulate matter at kerbside, urban, rural and background sites in Europe, *Atmos. Environ.*,  
1085 38(16), 2579–2595, doi:http://dx.doi.org/10.1016/j.atmosenv.2004.01.041, 2004.
- 1086 Putaud, J.-P., Van Dingenen, R., Alastuey, A., Bauer, H., Birmili, W., Cyrus, J., Flentje, H., Fuzzi, S., Gehrig, R.,  
1087 Hansson, H. C., Harrison, R. M., Herrmann, H., Hitzenberger, R., Hüglin, C., Jones, A. M., Kasper-Giebl, A., Kiss,  
1088 G., Kousa, A., Kuhlbusch, T. A. J., Löschau, G., Maenhaut, W., Molnar, A., Moreno, T., Pekkanen, J., Perrino, C.,  
1089 Pitz, M., Puxbaum, H., Querol, X., Rodriguez, S., Salma, I., Schwarz, J., Smolik, J., Schneider, J., Spindler, G., ten  
1090 Brink, H., Tursic, J., Viana, M., Wiedensohler, A., and Raes, F.: A European aerosol phenomenology – 3: Physical  
1091 and chemical characteristics of particulate matter from 60 rural, urban, and kerbside sites across Europe, *Atmos.*  
1092 *Environ.*, 44(10), 1308–1320, doi:10.1016/j.atmosenv.2009.12.011, 2010.
- 1093 Quincey, P., Butterfield, D., Green, D., Coyle, M., and Cape, J. N.: An evaluation of measurement methods for  
1094 organic, elemental and black carbon in ambient air monitoring sites, *Atmos. Environ.*, 43(32), 5085–5091,  
1095 doi:http://dx.doi.org/10.1016/j.atmosenv.2009.06.041, 2009.
- 1096 Ram, K., Sarin, M. M., and Tripathi, S. N.: Temporal Trends in Atmospheric PM<sub>2.5</sub>, PM<sub>10</sub>, Elemental Carbon,  
1097 Organic Carbon, Water-Soluble Organic Carbon, and Optical Properties: Impact of Biomass Burning Emissions in  
1098 The Indo-Gangetic Plain, *Environ. Sci. Technol.*, 46(2), 686–695, doi:10.1021/es202857w, 2012.
- 1099 Remoundaki, E., Kassomenos, P., Mantas, E., Mihalopoulos, N., and Tsezos, M.: Composition and Mass Closure of  
1100 PM<sub>2.5</sub> in Urban Environment (Athens, Greece), *Aerosol Air Qual. Res.*, 13(1), 72–82, 2013.
- 1101 Rickards, A. M. J., Miles, R. E. H., Davies, J. F., Marshall, F. H., and Reid, J. P.: Measurements of the Sensitivity of  
1102 Aerosol Hygroscopicity and the  $\kappa$  Parameter to the O/C Ratio, *J. Phys. Chem. A*, 117(51), 14120–14131,  
1103 doi:10.1021/jp407991n, 2013.
- 1104 Robinson, C. B., Schill, G. P., Zarzana, K. J., and Tolbert, M. A.: Impact of Organic Coating on Optical Growth of  
1105 Ammonium Sulfate Particles, *Environ. Sci. Technol.*, 47(23), 13339–13346, doi:10.1021/es4023128, 2013.

- 1106 Santoso, M., Dwiana Lestiani, D., and Hopke, P. K.: Atmospheric black carbon in PM<sub>2.5</sub> in Indonesian cities, *J. Air*  
 1107 *Waste Manage. Assoc.*, 63(9), 1022–1025, doi:10.1080/10962247.2013.804465, 2013.
- 1108 Snider, G., Weagle, C. L., Martin, R. V., van Donkelaar, A., Conrad, K., Cunningham, D., Gordon, C., Zwicker, M.,  
 1109 Akoshile, C., Artaxo, P., Anh, N. X., Brook, J., Dong, J., Garland, R. M., Greenwald, R., Griffith, D., He, K.,  
 1110 Holben, B. N., Kahn, R., Koren, I., Lagrosas, N., Lestari, P., Ma, Z., Vanderlei Martins, J., Quel, E. J., Rudich, Y.,  
 1111 Salam, A., Tripathi, S. N., Yu, C., Zhang, Q., Zhang, Y., Brauer, M., Cohen, A., Gibson, M. D., and Liu, Y.:  
 1112 SPARTAN: a global network to evaluate and enhance satellite-based estimates of ground-level particulate matter for  
 1113 global health applications, *Atmos. Meas. Tech.*, 8(1), 505–521, doi:10.5194/amt-8-505-2015, 2015.
- 1114 Sorooshian, A., Hersey, S., Brechtel, F. J., Corless, A., Flagan, R. C., and Seinfeld, J. H.: Rapid, Size-Resolved  
 1115 Aerosol Hygroscopic Growth Measurements: Differential Aerosol Sizing and Hygroscopicity Spectrometer Probe  
 1116 (DASH-SP), *Aerosol Sci. Technol.*, 42(6), 445–464, doi:10.1080/02786820802178506, 2008.
- 1117 Sun, Y.-L., Zhang, Q., Schwab, J. J., Demerjian, K. L., Chen, W.-N., Bae, M.-S., Hung, H.-M., Hogrefe, O., Frank,  
 1118 B., Rattigan, O. V., and Lin, Y.-C.: Characterization of the sources and processes of organic and inorganic aerosols  
 1119 in New York city with a high-resolution time-of-flight aerosol mass spectrometer, *Atmos. Chem. Phys.*, 11(4),  
 1120 1581–1602, doi:10.5194/acp-11-1581-2011, 2011.
- 1121 Svenningsson, B., Rissler, J., Swietlicki, E., Mircea, M., Bilde, M., Facchini, M. C., Decesari, S., Fuzzi, S., Zhou, J.,  
 1122 Mønster, J., and Rosenørn, T.: Hygroscopic growth and critical supersaturations for mixed aerosol particles of  
 1123 inorganic and organic compounds of atmospheric relevance, *Atmos. Chem. Phys.*, 6(7), 1937–1952,  
 1124 doi:10.5194/acp-6-1937-2006, 2006.
- 1125 Swietlicki, E., Hansson, H.-C., Hämeri, K., Svenningsson, B., Massling, A., McFiggans, G., McMurry, P. H., Petäjä,  
 1126 T., Tunved, P., Gysel, M., Topping, D., Weingartner, E., Baltensperger, U., Rissler, J., Wiedensohler, A., and  
 1127 Kulmala, M.: Hygroscopic properties of submicrometer atmospheric aerosol particles measured with H-TDMA  
 1128 instruments in various environments—a review, *Tellus B*, 60(3), 432–469, 2008.
- 1129 Taha, G., Box, G. P., Cohen, D. D., and Stelcer, E.: Black Carbon Measurement using Laser Integrating Plate  
 1130 Method, *Aerosol Sci. Technol.*, 41(3), 266–276, doi:10.1080/02786820601156224, 2007.
- 1131 USEPA: Chemical Speciation Network Database, [online] Available from:  
 1132 <http://views.cira.colostate.edu/fed/DataWizard/Default.aspx> (Accessed 1 December 2015), 2015.
- 1133 Varutbangkul, V., Brechtel, F. J., Bahreini, R., Ng, N. L., Keywood, M. D., Kroll, J. H., Flagan, R. C., Seinfeld, J.  
 1134 H., Lee, A., and Goldstein, A. H.: Hygroscopicity of secondary organic aerosols formed by oxidation of  
 1135 cycloalkenes, monoterpenes, sesquiterpenes, and related compounds, *Atmos. Chem. Phys.*, 6(9), 2367–2388,  
 1136 doi:10.5194/acp-6-2367-2006, 2006.
- 1137 Villalobos, A. M., Amonov, M. O., Shafer, M. M., Devi, J. J., Gupta, T., Tripathi, S. N., Rana, K. S., Mckenzie, M.,  
 1138 Bergin, M. H., and Schauer, J. J.: Source apportionment of carbonaceous fine particulate matter (PM<sub>2.5</sub>) in two  
 1139 contrasting cities across the Indo-Gangetic Plain, *Atmos. Pollut. Res.*, 6(3), 398, 2015.
- 1140 Vu Van, H., Le Xuan, Q., Pham Ngoc, H., and Luc, H.: Health Risk Assessment of Mobility-Related Air Pollution  
 1141 in Ha Noi, Vietnam, *J. Environ. Prot. (Irvine, Calif.)*, 4(10), 1165–1172, 2013.
- 1142 Wagner, F., Bortoli, D., Pereira, S., João Costa, M., Silva, A. M., Weinzierl, B., Esselborn, M., Petzold, A., Rasp,  
 1143 K., Heinold, B., and Tegen, I.: Properties of dust aerosol particles transported to Portugal from the Sahara desert,  
 1144 *Tellus B*, 61(1), 297–306, 2009.
- 1145 Wang, J. L.: Mapping the Global Dust Storm Records: Review of Dust Data Sources in Supporting  
 1146 Modeling/Climate Study, *Curr. Pollut. Reports*, 1(2), 82–94, doi:10.1007/s40726-015-0008-y, 2015.
- 1147 Wang, Z., Chen, L., Tao, J., Zhang, Y., and Su, L.: Satellite-based estimation of regional particulate matter (PM) in  
 1148 Beijing using vertical-and-RH correcting method, *Remote Sens. Environ.*, 114(1), 50–63,  
 1149 doi:<http://dx.doi.org/10.1016/j.rse.2009.08.009>, 2010.
- 1150 Wexler, A. S. and Clegg, S. L.: Atmospheric aerosol models for systems including the ions H<sup>+</sup>, NH<sub>4</sub><sup>+</sup>, Na<sup>+</sup>, SO<sub>4</sub><sup>2-</sup>,  
 1151 NO<sub>3</sub><sup>-</sup>, Cl<sup>-</sup>, Br<sup>-</sup>, and H<sub>2</sub>O, *J. Geophys. Res. Atmos.*, 107(D14), ACH14–1–14, doi:10.1029/2001JD000451, 2002.
- 1152 WHO: Human exposure to air pollution, in Update of the World Air Quality Guidelines World Health Organization,

- 1153 pp. 61–86, World Health Organization, Geneva, Switzerland., 2005.
- 1154 WHO: WHO | Air quality guidelines - global update 2005, World Health Organization, Geneva, Switzerland., 2006.
- 1155 Wise, M. E., Surratt, J. D., Curtis, D. B., Shilling, J. E., and Tolbert, M. A.: Hygroscopic growth of ammonium  
1156 sulfate/dicarboxylic acids, *J. Geophys. Res. Atmos.*, 108(D20), 4638, doi:10.1029/2003JD003775, 2003.
- 1157 Yang, F., Tan, J., Zhao, Q., Du, Z., He, K., Ma, Y., Duan, F., and Chen, G.: Characteristics of PM<sub>2.5</sub> speciation in  
1158 representative megacities and across China, *Atmos. Chem. Phys.*, 11(11), 5207–5219, doi:10.5194/acp-11-5207-  
1159 2011, 2011.
- 1160 Zhang, R., Jing, J., Tao, J., Hsu, S.-C., Wang, G., Cao, J., Lee, C. S. L., Zhu, L., Chen, Z., Zhao, Y., and Shen, Z.:  
1161 Chemical characterization and source apportionment of PM<sub>2.5</sub> in Beijing: seasonal perspective, *Atmos. Chem. Phys.*,  
1162 13(14), 7053–7074, doi:10.5194/acp-13-7053-2013, 2013.
- 1163 Zhang, W.-J., Sun, Y.-L., Zhuang, G.-S., and Xu, D.-Q.: Characteristics and seasonal variations of PM<sub>2.5</sub>, PM<sub>10</sub>,  
1164 and TSP aerosol in Beijing, *Biomed. Environ. Sci.*, 19(6), 461–468, 2006.
- 1165
- 1166



1167 **Figures and Tables**

1168 **Table 1: Summary of speciation definitions**

Species (at 0% RH)	Measurement Method	Species Mass ( $\mu\text{g}$ ). For concentrations, divide masses by sampling volume $v$	Reference
SS	IC (anion and cation)	$2.54[\text{Na}^+]_{\text{SS}}$ , where $[\text{Na}^+]_{\text{SS}} = [\text{Na}^+]_{\text{tot}} - 0.1[\text{Al}]$	(Remoundaki et al., 2013) (Malm et al., 1994)
ANO <sub>3</sub>		$1.29[\text{NO}_3^-]$	(Malm et al., 1994)
ASO <sub>4</sub>		$[\text{SO}_4^{2-}]_{\text{non-ss}} + [\text{NH}_4^+] - 0.29[\text{NO}_3^-]$ , where $[\text{SO}_4^{2-}]_{\text{non-ss}} = [\text{SO}_4^{2-}]_{\text{total}} - 0.12[\text{Na}^+]$	(Dabek-Zlotorzynska et al., 2011; Henning et al., 2003)
Na <sub>2</sub> SO <sub>4</sub>		$0.18[\text{Na}^+]_{\text{SS}}$	
CM	ICP-MS & IC	$10 \times ([\text{Al}] + [\text{Mg}] + [\text{Fe}])$	(Wang, 2015)
EBC	SSR	$20.7 \times \ln(R_o/R)$	(Taha et al., 2007)
TEO	ICP-MS	$1.47[\text{V}] + 1.27[\text{Ni}] + 1.25[\text{Cu}] + 1.24[\text{Zn}] + 1.32[\text{As}] + 1.2[\text{Se}] + 1.07[\text{Ag}] + 1.14[\text{Cd}] + 1.2[\text{Sb}] + 1.12[\text{Ba}] + 1.23[\text{Ce}] + 1.08[\text{Pb}]$	(Malm et al., 1994)
PBW <sub>inorg</sub>	$\kappa_{m,X}$	$\sum_X [f_{m,X}(\text{RH}) - 1][X]$	(Kreidenweis et al., 2008)
PBW <sub>RM</sub>		$\text{RM}(1 - 1/f_{m,\text{RM}})$	Table 2
RM(35%)	Mass Balance	$[\text{PM}_{2.5}] - \{[\text{EBC}] + [\text{CM}] + [\text{TEO}] + [\text{ANO}_3] + [\text{SS}] + [\text{ASO}_4] + [\text{Na}_2\text{SO}_4] + [\text{PBW}]_{\text{inorg}}\}$	This Study
RM(0%)	Mass Balance $\kappa_{m,\text{OM}} = 0.07$	$\text{RM}(35\%) - \text{PBW}_{\text{RM}}$	Organic growth factors: (Jimenez et al., 2009; Sun et al., 2011)

1169 **Species:** EBC = Equivalent black carbon, TEO = Trace metal oxides, CM = Crustal Material, ANO<sub>3</sub> = Ammonium  
 1170 nitrate, ASO<sub>4</sub> = **Ammoniated** sulfate, PBW = particle-bound water, RM = **residual** matter (assumed representative of  
 1171 organic matter), [X] = concentration of any hygroscopic species. **Measurement Instruments:** IC = Ion  
 1172 Chromatography, ICP-MS Inductively coupled plasma mass spectrometry, SSR = Smoke Stain Reflectometer,  $\kappa_{m,X}$   
 1173 = single-parameter hygroscopicity by mass (Kreidenweis et al., 2008). RH = Relative Humidity,

1174

1175 **Table 2:  $\kappa$ -Kohler constants for volume ( $\kappa_v$ ), mass ( $\kappa_m$ ), and related quantities**

Compound [X]	$\kappa_{v,X}$	Approximate Density ( $\rho_X/\rho_{\text{water}}$ )	$\kappa_{m,X}$	PBW(% mass) at	
				RH = 35%	RH = 80%
Crustal	0	2.5 <sup>a</sup>	0	0	0
EBC	0	1.8 <sup>b</sup>	0	0	0
TEO	0	2.5	0	0	0
RM	0.1 <sup>c</sup>	1.4	0.07	2	12
ANO <sub>3</sub>	0.41	1.72	0.24	17	61
ASO <sub>4</sub>	0.51	1.76	0.29	15	56
Na <sub>2</sub> SO <sub>4</sub>	0.68 <sup>d</sup>	2.68 <sup>d</sup>	0.25	12	50
SS	1.5 <sup>e</sup>	2.16	0.69	22	68

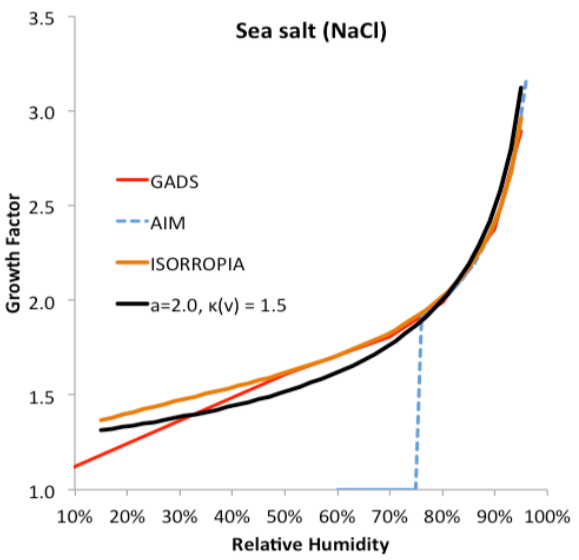
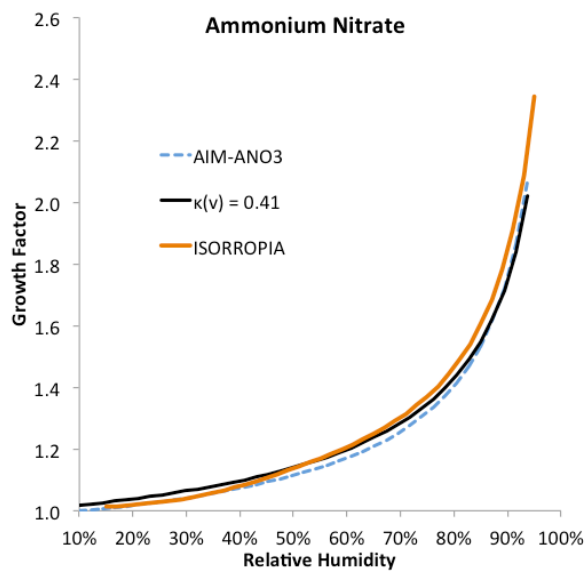
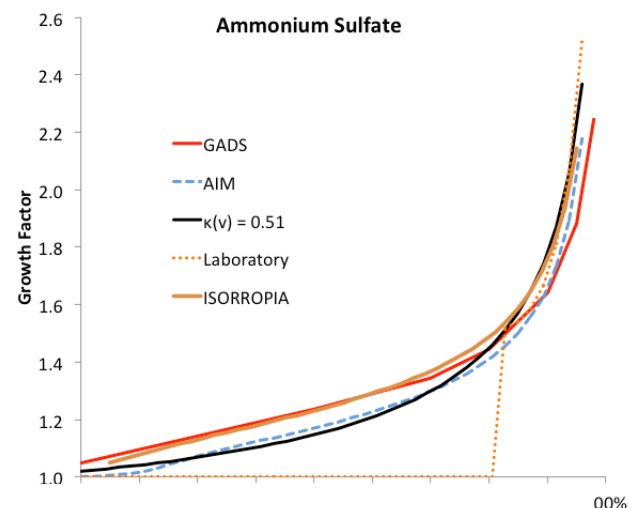
1176 PBW = Particle-bound water. EBC = Equivalent black carbon, TEO = Trace Element Oxides, RM = Residue Matter  
 1177 (associated with organics), ANO<sub>3</sub> = ammonium nitrate, ASO<sub>4</sub> = **Ammoniated** sulfate. <sup>a</sup>Wagner et al. (2009), <sup>b</sup>Bond  
 1178 and Bergstrom (2006), <sup>c</sup>Assuming an urban O:C ratio of 0.5 then  $\kappa_{v,\text{OM}} = 0.1$  Jimenez et al. (2009), <sup>d</sup>Petters and  
 1179 Kreidenweis (2007). <sup>e</sup>Fitted using non-deliqesced, subsaturated AIM Model III values, plus 0% RH endpoint by  
 1180 Kreidenweis et al. (2008).

1181

**Table 3: PM<sub>2.5</sub> composition and water content ( $\mu\text{g m}^{-3}$ ) at each SPARTAN location.**

City	Host Institute	Lat/Lon (°)	Elev./Inst. Elev. (m)	Filters (n)	ASO <sub>4</sub>	ANO <sub>3</sub>	CM	SS	EBC	TEO	RM	PBW 35%RH	$\rho$ 0%RH (g/cm <sup>3</sup> )	NO <sub>3</sub> vs. NH <sub>4</sub> <sup>+</sup> (r)	PM <sub>2.5</sub>	PM <sub>2.5</sub> /PM <sub>10</sub>	$\kappa_{p,loc}$	PM <sub>2.5</sub> K/Al	Zn/Al	Filter Sampling Period
Beijing	Tsinghua University	40.010, 116.333	60//7.5	114	12.0 (7.9)	5.5 (6.4)	15.9 (8.8)	1.5 (2.1)	5.7 (3.4)	0.62 (0.51)	23.8 (18)	4.7 (2.8)	1.69	0.32	69.5 (2.5)	0.49	0.19	2.9	0.51	2013/06–2016/02
Bandung	ITB Bandung	-6.888, 107.610	826//20	77	6.0 (2.3)	0.7 (1.3)	2.5 (1.5)	0.3 (0.2)	3.7 (2.0)	0.14 (0.11)	16.0 (5.9)	1.9 (0.6)	1.55	0.06	31.4 (1.0)	0.58	0.17	6.8	0.52	2014/01–2015/11
Manila	Manila Observatory	14.635, 121.080	60//10	63	2.7 (1.5)	0.3 (0.2)	1.9 (1.0)	0.5 (0.4)	4.3 (3.3)	0.13 (0.13)	7.3 (3.5)	1.1 (0.5)	1.61	0.03	18.2 (0.8)	0.39	0.16	6.3	1.03	2014/02–
Dhaka	Dhaka University	23.728, 90.398	20//20	41	7.5 (4.3)	2.1 (1.8)	5.9 (4.0)	1.4 (1.7)	8.4 (5.1)	1.50 (1.46)	21.4 (16)	3.5 (2.2)	1.63	0.43	51.9 (3.7)	0.40	0.17	5.3	3.39	2016/01–2015/11
Ilorin	Ilorin University	8.484, 4.675	330//10	40	1.9 (0.8)	0.3 (0.1)	3.0 (2.2)	0.3 (0.4)	1.6 (0.8)	0.09 (0.07)	7.6 (3.8)	0.9 (0.4)	1.62	0.05	15.7 (0.8)	0.44	0.15	2.9	0.49	2014/03–
Kanpur	IIT Kanpur	26.519, 80.233	130//10	33	17.6 (12)	6.8 (5.3)	4.4 (2.3)	0.6 (0.3)	8.3 (4.7)	0.47 (0.36)	54.6 (33)	6.3 (3.6)	1.52	0.58	99.3 (9.1)	0.56	0.18	16.2	1.01	2015/10–2013/12
Buenos Aires	CITEDEF	-34.560, -58.506	25//7	31	1.1 (0.5)	0.8 (0.4)	2.2 (1.6)	0.6 (0.3)	1.7 (1.2)	0.12 (0.12)	3.1 (1.8)	0.9 (0.3)	1.70	0.28	10.1 (0.6)	0.39	0.19	2.7	0.44	2014/11–2014/10
Rehovot	Weizmann Institute	31.907, 34.810	20//10	30	4.7 (1.9)	0.9 (0.5)	3.3 (1.6)	0.7 (0.6)	2.2 (2.0)	0.12 (0.13)	2.6 (2.8)	1.6 (0.6)	1.79	0.01	16.1 (1.0)	0.40	0.28	2.7	0.40	2016/02–2015/02
Mammoth Cave NP	Mammoth Cave	37.132, -86.148	235//7	19	4.1 (2.4)	0.2 (0.1)	1.4 (1.4)	0.1 (0.1)	0.7 (0.4)	0.02 (0.03)	6.1 (4.3)	1.0 (0.5)	1.59	0.00	13.6 (1.8)	0.56	0.22	1.1	0.13	2014/04–2014/08
Atlanta	Emory University	33.688, -84.290	250//2	13	2.0 (0.9)	0.3 (0.1)	1.0 (0.4)	0.1 (0.1)	1.1 (1.0)	0.04 (0.02)	4.1 (1.8)	0.6 (0.2)	1.61	0.00	9.1 (0.7)	0.69	0.17	1.9	0.26	2014/01–2014/05
Singapore	NUS	1.298, 103.780	10//20	12	16.1 (6.5)	1.2 (0.9)	0.8 (0.3)	0.9 (0.4)	3.1 (2.7)	0.20 (0.16)	39.8 (29)	5.0 (2.4)	1.48	0.66	66.8 (11)	NA	0.21	13.2	1.53	2015/08–
Hanoi	Vietnam Acad. Sci.	21.048, 105.800	10//20	10	6.0 (2.1)	1.6 (0.4)	5.6 (5.4)	0.9 (0.2)	3.7 (2.1)	0.69 (0.43)	18.2 (7.8)	2.6 (0.7)	1.59	0.22	39.4 (3.9)	0.38	0.18	8.9	3.74	2015/12–2015/05
Pretoria	CSIR	-25.756, 28.280	1310//10	5	1.2 (1.6)	0.7 (0.3)	1.3 (1.8)	0.2 (0.1)	1.4 (0.9)	0.04 (0.04)	1.0 (0.7)	0.5 (0.4)	2.09	0.48	6.4 (2.3)	0.32	0.24	6.0	0.86	2015/09–2015/11
SPARTAN mean (% mass)	All sites			497	20 (11)%	4.7 (3.0)%	13.4 (9.9)%	2.3 (1.6)%	11.9 (8.4)%	1.0 (1.1)%	40 (24)%	7.2 (3.3)%	1.65	0.24	32.4 (2.9)	0.50	0.20	4.6	0.73	2013–2016

<sup>a</sup>Values in parentheses are 1 $\sigma$  standard deviations. RH = Relative Humidity, ANO<sub>3</sub> = ammonium nitrate, ASO<sub>4</sub> = Ammoniated sulfate, CM = Crustal material, EBC = Equivalent black carbon, TEO = Trace Element Oxides, RM = Residue Matter, PBW = Particle-bound water. Mean Na<sub>2</sub>SO<sub>4</sub> was not significant (< 0.1  $\mu\text{g m}^{-3}$ ) at any SPARTAN site. <sup>b</sup>Geometric mean of ratio



**Figure 1: Hygroscopic growth factors for ASO<sub>4</sub> (top), ANO<sub>3</sub> (centre), and sea salt (bottom). GADS = Global Aerosol Dataset estimated from empirical data (Koepke et al., 1997). ISORROPIA = Aerosol thermodynamic model at T=298K (reverse mode) and assuming linear water/solvent volume additivity (Fountoukis and Nenes, 2007). AIM = Aerosol Inorganic Model calculated metastable growth for ASO<sub>4</sub> and ANO<sub>3</sub> at T=298K (Wexler and Clegg, 2002), Laboratory ASO<sub>4</sub> fit is  $GF = 1.49 + 2.81 \cdot RH^{24.6}$  (with deliquescence at 80%) for bulk pure ASO<sub>4</sub> (Wise et al., 2003). All components are fit using Eq 6.**

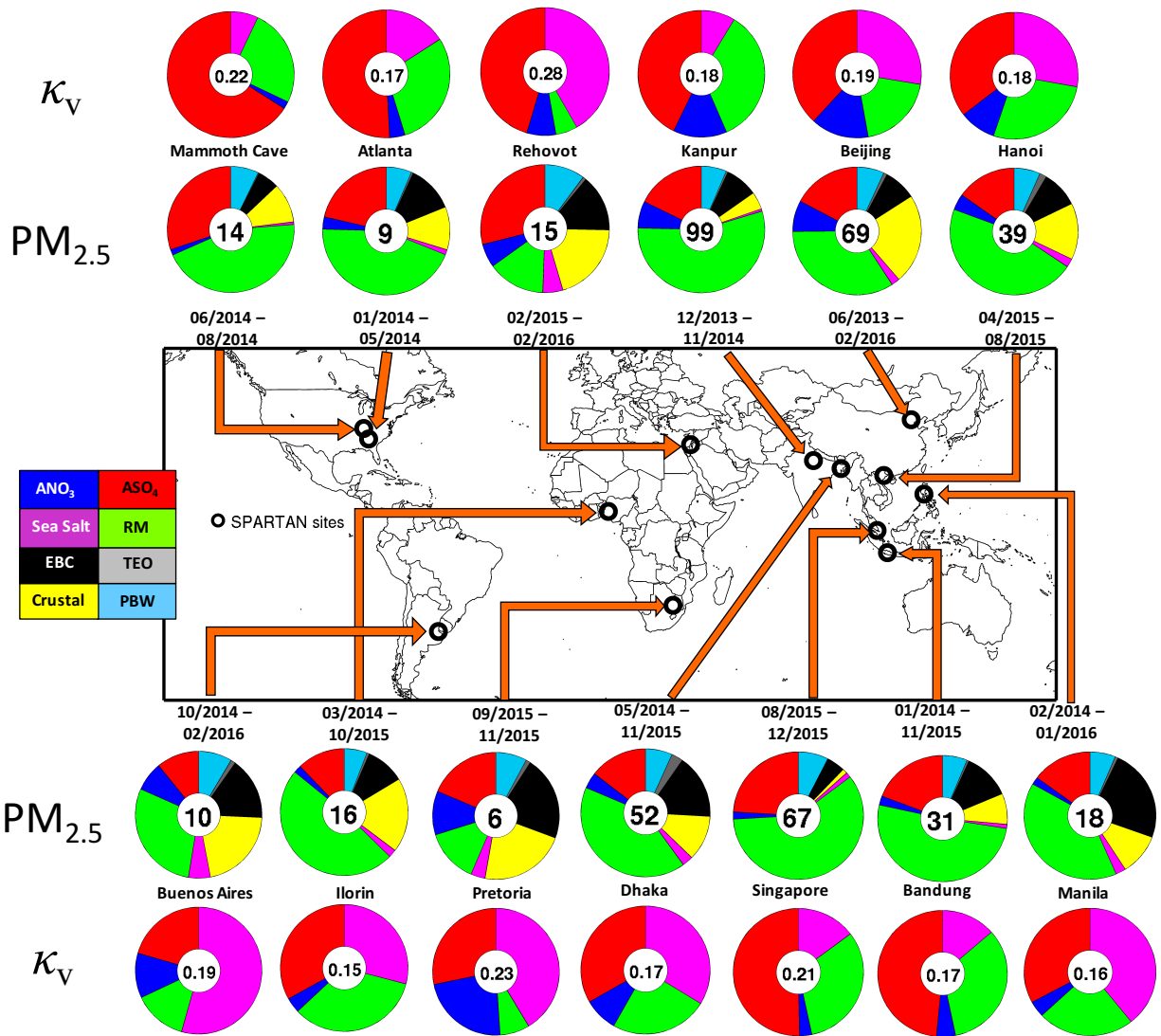




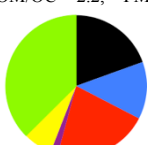

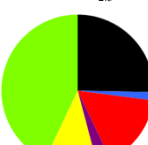
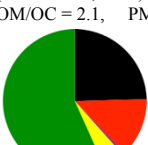
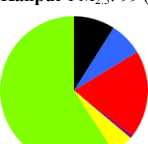
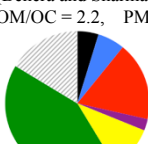
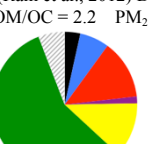
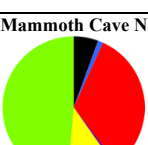
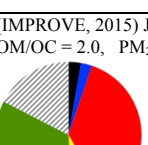
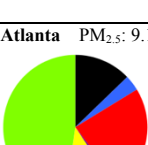
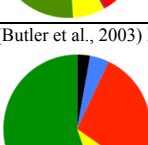
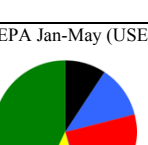
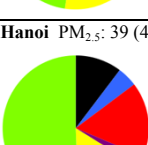
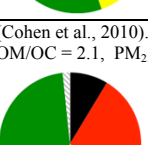
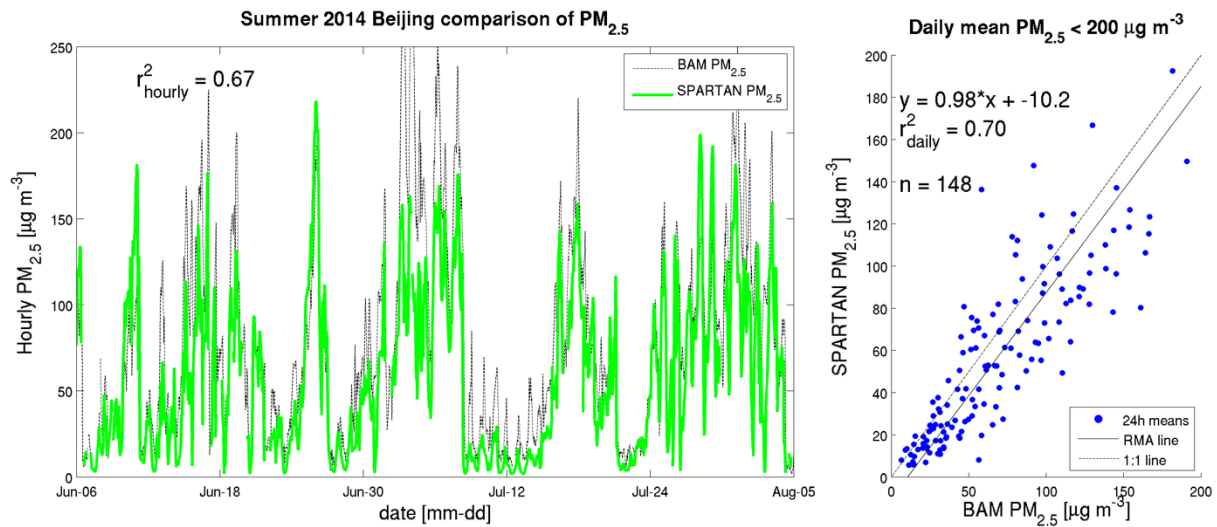


Figure 2: PM<sub>2.5</sub> mass (inner circle, μg m<sup>-3</sup>) and composition mass fraction (filled colors) is shown in interior pie charts. Exterior pie charts contain site-mean κ<sub>v</sub> surrounded by the relative contribution of PBW water at 35% RH.

Figure 3: Comparison of SPARTAN water-free aerosol composition with 11 collocated speciation studies. The numbers in parentheses show 1- $\sigma$  deviations of averaged masses. The number of filters sampled is  $n$ . Dark green = organic, Light green = residual, black = equivalent black carbon, red = Ammoniated sulfate, blue = ammonium nitrate, purple = sea salt, yellow = crustal, and grey stripes = unknown. OM/OC ratios are from Philip et al. (2014b) and Canagaratna et al. (2015). Relative mass percentages are based on water-free aerosol components. SPARTAN percentages are renormalized to 100% after omission of species not found in comparison studies.

PM <sub>2.5</sub> mass = $\mu\text{g m}^{-3}$ ( $1\sigma/\sqrt{n}$ ), components = % ( $1\sigma$ )		
This study (total mass = $\mu\text{g m}^{-3}$ )	Prior Study ( $\mu\text{g m}^{-3}$ )	Prior Study ( $\mu\text{g m}^{-3}$ )
<b>Beijing</b> PM <sub>2.5</sub> : 69 (3), $n = 114$  <ul style="list-style-type: none"> <li>8.5 (10)% ANO<sub>3</sub>,</li> <li>19 (12)% ASO<sub>4</sub>,</li> <li>2.3 (3.3)% SS,</li> <li>25 (14)% CM,</li> <li>8.8 (5.3)% EBC,</li> <li>37 (27)% RM</li> </ul>	(Yang et al., 2011) 2005-2006, OM/OC = 1.7, PM <sub>2.5</sub> : 119(40)  <ul style="list-style-type: none"> <li>11 (7)% ANO<sub>3</sub>,</li> <li>17 (10)% ASO<sub>4</sub>,</li> <li>1.3 (0.6)% SS,</li> <li>19 (3)% CM,</li> <li>7 (5)% EC,</li> <li>33 (16)% OM,</li> <li>10 (10)% Unk</li> </ul>	(Oanh et al., 2006) 2001-2004, OM/OC = 1.7 PM <sub>2.5</sub> : 136 (45)  <ul style="list-style-type: none"> <li>12 (1.5)% ANO<sub>3</sub>,</li> <li>20 (1.8)% ASO<sub>4</sub>,</li> <li>1.2 (1.2)% SS,</li> <li>5 (3)% CM,</li> <li>9 (7)% EBC,</li> <li>29 (22)% OM,</li> <li>24 (24)% Unk</li> </ul>
<b>Bandung</b> PM <sub>2.5</sub> : 31 (1), $n = 77$  <ul style="list-style-type: none"> <li>2.4 (1.4)% ANO<sub>3</sub>,</li> <li>21 (8)% ASO<sub>4</sub>,</li> <li>1.0 (0.3)% SS,</li> <li>8.6 (4.1)% CM,</li> <li>13 (4)% EBC,</li> <li>55 (19)% RM</li> </ul>	(Oanh et al., 2006) 2001-2004, OM/OC = 2.2, PM <sub>2.5</sub> : 45.5(10.6),  <ul style="list-style-type: none"> <li>13(4)% ANO<sub>3</sub>,</li> <li>21(3)% ASO<sub>4</sub>,</li> <li>1.6(0.2)% SS,</li> <li>6.6(0.5)% CM,</li> <li>19 (4)% EBC,</li> <li>36(11)% RM</li> </ul>	(Lestari and Mauliadi, 2009) 2001- 2007, OM/OC = 2.2 PM <sub>2.5</sub> : 43.5(10.5)  <ul style="list-style-type: none"> <li>4(6)% ANO<sub>3</sub>,</li> <li>4(4)% ASO<sub>4</sub>,</li> <li>3(2)% SS,</li> <li>23(21)% CM,</li> <li>24(14)% EBC,</li> <li>42(35)% RM</li> </ul>
<b>Manila</b> PM <sub>2.5</sub> : 18 (1), $n = 63$  <ul style="list-style-type: none"> <li>1.8 (1.2)% ANO<sub>3</sub>,</li> <li>16 (9)% ASO<sub>4</sub>,</li> <li>2.9 (2.4)% SS,</li> <li>11 (6)% CM,</li> <li>25 (19)% EBC,</li> <li>43 (21)% RM</li> </ul>	(Cohen et al., 2009) 2001-2007, OM/OC = 2.1, PM <sub>2.5</sub> : 46 (19),  <ul style="list-style-type: none"> <li>ANO<sub>3</sub> N/A</li> <li>14 (9)% ASO<sub>4</sub>,</li> <li>0.6 (1.5)% SS,</li> <li>5 (1.7)% CM,</li> <li>25 (11)% EBC,</li> <li>57(22)% OM,</li> </ul>	
<b>Kanpur</b> PM <sub>2.5</sub> : 99 (9), $n = 33$  <ul style="list-style-type: none"> <li>7.4 (5.7)% ANO<sub>3</sub>,</li> <li>19 (13)% ASO<sub>4</sub>,</li> <li>0.7 (0.3)% SS,</li> <li>4.8 (2.9)% CM,</li> <li>9 (5.0)% EBC,</li> <li>59 (35)% RM</li> </ul>	(Behera and Sharma, 2010) Oct. 2007 – Jan 2008, OM/OC = 2.2, PM <sub>2.5</sub> : 172 (73),  <ul style="list-style-type: none"> <li>6.1 (1.3)% ANO<sub>3</sub>,</li> <li>18 (4)% ASO<sub>4</sub>,</li> <li>2.6 (0.6)% SS,</li> <li>10 (3)% CM,</li> <li>4.8 (1.1)% EC,</li> <li>42 (9)% OM,</li> <li>16 (10)% Unk</li> </ul>	(Ram et al., 2012) Dec 2008 – Feb 2009, OM/OC = 2.2 PM <sub>2.5</sub> : 158 (47)  <ul style="list-style-type: none"> <li>6.6(4)% ANO<sub>3</sub>,</li> <li>13 (5)% ASO<sub>4</sub>,</li> <li>1.5 (0.9)% SS,</li> <li>12 (6)% CM*</li> <li>3 (1.1)% EC,</li> <li>57 (23)% OM,</li> <li>6 (24)% Unk</li> </ul> <p>*Assuming CM = [Ca]/0.034 (Wang, 2015)</p>
<b>Mammoth Cave NP</b> PM <sub>2.5</sub> : 13.6 (2), $n = 19$  <ul style="list-style-type: none"> <li>1.2 (1.0)% ANO<sub>3</sub>,</li> <li>33 (19)% ASO<sub>4</sub>,</li> <li>0.8 (0.8)% SS,</li> <li>11 (11)% CM,</li> <li>5.6 (3.2)% EBC,</li> <li>49 (34)% RM</li> </ul>	(IMPROVE, 2015) June-Aug. 2014, OM/OC = 2.0, PM <sub>2.5</sub> : 10.0 (5.8),  <ul style="list-style-type: none"> <li>2.4 (2.5)% ANO<sub>3</sub>,</li> <li>36 (17)% ASO<sub>4</sub>,</li> <li>0.3 (1.6)% SS,</li> <li>7 (8)% CM,</li> <li>3 (3)% EC,</li> <li>34 (30)% OM,</li> <li>17% Unk+H<sub>2</sub>O</li> </ul>	
<b>Atlanta</b> PM <sub>2.5</sub> : 9.1 (1), $n = 13$  <ul style="list-style-type: none"> <li>3.5 (1.2)% ANO<sub>3</sub>,</li> <li>23 (11)% ASO<sub>4</sub>,</li> <li>1.2 (1.2)% SS,</li> <li>12 (4.7)% CM,</li> <li>11 (2.6)% EBC,</li> <li>48 (25)% RM</li> </ul>	(Butler et al., 2003) Mar. 1999 –2000 Feb, OM/OC = 2.0, PM <sub>2.5</sub> : 24.2  <ul style="list-style-type: none"> <li>4 (0.2)% ANO<sub>3</sub>,</li> <li>28 (1.0)% ASO<sub>4</sub>,</li> <li>10 (0.8)% CM,</li> <li>3 (0.2)% EC,</li> <li>55 (5)% OM,</li> </ul>	EPA Jan-May (USEPA, 2015), OM/OC = 2.0 PM <sub>2.5</sub> : 8.5  <ul style="list-style-type: none"> <li>12 (5)% ANO<sub>3</sub>,</li> <li>23 (15)% ASO<sub>4</sub>,</li> <li>1.4 (0.6)% SS</li> <li>12 (5)% CM,</li> <li>9.3 (5)% EC,</li> <li>43 (36)% OM,</li> </ul>
<b>Hanoi</b> PM <sub>2.5</sub> : 39 (4), $n = 10$  <ul style="list-style-type: none"> <li>4.4 (1.1)% ANO<sub>3</sub>,</li> <li>17 (6)% ASO<sub>4</sub>,</li> <li>2.5 (0.6)% SS,</li> <li>16 (15)% CM,</li> <li>10 (5.8)% EBC,</li> <li>51 (22)% RM</li> </ul>	(Cohen et al., 2010). 2001 –2008 OM/OC = 2.1, PM <sub>2.5</sub> : 54 (33)  <ul style="list-style-type: none"> <li>ANO<sub>3</sub> N/A</li> <li>29 (20)% ASO<sub>4</sub>,</li> <li>0.6 (1.4)%SS</li> <li>13 (7)% CM,</li> <li>8 (3)% EBC,</li> <li>40 (19)% OM,</li> <li>2 (2)% Unk + ANO<sub>3</sub></li> </ul>	



**Figure 4: Left Hourly PM<sub>2.5</sub> estimated from SPARTAN overlaid with a MetOne BAM-1020 (June-August 2014) at the Beijing US Embassy (15 km away). Right: 24-hour SPARTAN PM<sub>2.5</sub> compared with BAM for the year 2014. Reduced major axis (RMA) slope and Pearson correlations for PM<sub>2.5</sub> are given in inset.**

## Appendix:

### Appendix A1:

**Table A1: Hygroscopicity parameter  $\kappa_v$  for various studies on organic material**

$\kappa_v$ (OM)	Comments	Reference
<b>0.045</b>	Fitted to an aged organic mixture, subsaturated	(Varutbangkul et al., 2006)
<b>0</b>	IMPROVE network, subsaturated	(Hand and Malm, 2006)
<b>0.10 ± 0.04</b>	RH > 99%, fitted to SOA precursors	(Prenni et al., 2007)
<b>-0.067 + 0.33(O:C)</b>	Fitted, RH > 99%	(Jimenez et al., 2009)
<b>0.29(O:C)</b>	RH > 99%, 0.3 < O:C < 0.6	(Chang et al., 2010)
<b>0.05</b>	Best estimate from aged mixtures, subsaturated	(Dusek et al., 2011)
<b>0.01 – 0.2</b>	Field studies & smog chamber, subsaturated	(Duplissy et al., 2011)
<b>0.16</b>	RH > 99%	(Asa-Awuku et al., 2011)
<b>0.05 – 0.13</b>	Lab experiments, aged with H <sub>2</sub> O <sub>2</sub> and light; subsaturated	(Liu et al., 2012)
<b>0.1</b>	RH > 99%, D <sub>dry</sub> < 100 nm	(Padró et al., 2012)
<b>0.12<math>\epsilon_{\text{WSOM}}^{\#}</math></b>	RH > 99%	(Lathem et al., 2013)
<b>-0.005 + 0.19(O:C)</b>	Fitted, RH > 99% 100 nm particle	(Rickards et al., 2013)
<b>0.03, 0.1</b>	HDTMA-measure, subsaturated	(Bezantakos et al., 2013)
<b>0.1</b>	Subsaturated	Selected for this study

<sup>#</sup> $\epsilon_{\text{WSOM}}$  = fraction of water-soluble organic material.

## Appendix A2:

Dry aerosol scatter ( $b_{sp,dry}$ ) is related to relative humidity (RH) by

$$b_{sp,dry} = \frac{b_{sp}(RH)}{f_v(RH)} \quad \text{Eq. A1}$$

Changes in scatter are also proportional to mass (Chow et al., 2006; Wang et al., 2010)

$$b_{sp,dry} = \alpha PM_{2.5,dry} \quad \text{Eq. A2}$$

where  $\alpha$  ( $m^2 g^{-1}$ ) is the mass scattering efficiency and a function of aerosol size distribution, effective radius, and dry composition. In this study we treat composition, density, and size distribution as constant over each of our 9-day intermittent sampling periods so that  $\alpha \approx \langle \alpha \rangle_{9d}$ . Under this assumption the predicted mass changes in low humidity (35% RH) are proportional to water-free aerosol scatter:

$$PM_{2.5,dry} = \langle PM_{2.5,dry} \rangle \frac{b_{sp,dry}}{\langle b_{sp,dry} \rangle} \quad \text{Eq. A3}$$

where  $\langle \rangle$  indicates 9-day averages. The explicit compensation for aerosol water is then

$$[PM_{2.5,dry}] = \frac{\langle [PM_{2.5,dry}] \rangle}{\langle b_{sp}(RH)/f_v(RH) \rangle} \cdot \frac{b_{sp}(RH)}{f_v(RH)} \quad \text{Eq. A4}$$

where  $[\ ]$  indicates concentration in  $\mu g m^{-3}$ . Uncertainties are a function of replicate weighing measurements ( $\pm 4 \mu g$ ), flow volume ( $\pm 10\%$ ), %RH ( $\pm 2.5$ ), aerosol scatter ( $\pm 5\%$ ), and  $\kappa_v$  ( $\pm 0.05$ ).

$$\left( \frac{\delta[PM_{2.5,h}]}{[PM_{2.5,h}]} \right)^2 \approx \left( \frac{\delta PM_{2.5}}{PM_{2.5}} \right)^2 + \left( \frac{\delta V}{V} \right)^2 + \left( \frac{\delta b_{sp}}{b_{sp}} \right)^2 + \left( \frac{\delta f_v}{f_v} \right)^2 \quad \text{Eq. A5}$$

where

$$\left( \frac{\delta f_v}{f_v} \right)^2 = \frac{(f_v - 1)^2}{f_v^2} \left[ \left( \frac{\delta \kappa}{\kappa} \right)^2 + \left( \frac{\delta RH}{RH \cdot (100 - RH)} \right)^2 \right] \quad \text{Eq. A6}$$

The average relative 2- $\sigma$   $PM_{2.5}$  uncertainty was 26% for dry hourly predictions, increasing with higher RH cutoffs. A cut-off of RH = 80% has been applied to our data, above which hygroscopic uncertainties, as well as total water mass, dominate.